MANUSCRIPT TITLE

Affinity-tagged SMAD1 and SMAD5 mouse lines reveal transcriptional reprogramming mechanisms during early pregnancy

AUTHORS

Zian Liao[a,b,c,d], Suni Tang[a,d], Kaori Nozawa[a,d], Keisuke Shimada[e], Masahito Ikawa[e], Diana Monsivais*[a,d], and Martin M. Matzuk*[a,b,c,d]

[a]Department of Pathology & Immunology, Baylor College of Medicine, Houston, TX, 77030, USA
[b]Department of Molecular and Human Genetics, Baylor College of Medicine, Houston, TX, 77030, USA
[c]Graduate Program of Genetics and Genomics, Baylor College of Medicine, Houston, TX, 77030, USA
[d]Center for Drug Discovery, Baylor College of Medicine, Houston, TX, 77030, USA
[e]Research Institute for Microbial Diseases, Osaka University, Osaka, 565-0871, Japan

*To whom correspondence should be addressed to: Martin M. Matzuk, MD, PhD Tel: +1 713-798-6451; Fax: +1 713-798-5838; Email: mmatzuk@bcm.edu; and Diana Monsivais, PhD Tel: +1 713-798-1279; Fax: +1 713-798-5838; Email: diana.monsivais@bcm.edu.

KEY WORDS: uterus, decidualization, SMAD proteins, bone morphogenetic proteins, progesterone, endometrium

ABSTRACT

Endometrial decidualization, a prerequisite for successful pregnancies, relies on transcriptional reprogramming driven by progesterone receptor (PR) and bone morphogenetic protein (BMP)-SMAD1/SMAD5 signaling pathways. Despite their critical roles in early pregnancy, how these pathways intersect in reprogramming the endometrium into a receptive state remains unclear. To define how SMAD1 and/or SMAD5 integrate BMP signaling in the uterus during early pregnancy, we generated two novel transgenic mouse lines with affinity tags inserted into the endogenous SMAD1 and SMAD5 loci (*Smad1*$^{HA/HA}$ and *Smad5*$^{PA/PA}$). By profiling the genome-wide distribution of SMAD1, SMAD5, and PR in the mouse uterus, we demonstrated the unique and shared roles of SMAD1 and SMAD5 during the window of implantation. We also showed the presence of a conserved SMAD1, SMAD5, and PR genomic binding signature in the uterus during early pregnancy. To functionally characterize the translational aspects of our findings, we demonstrated that SMAD1/5 knockdown in human endometrial stromal cells suppressed expressions of canonical decidual markers (*IGFBP1, PRL, FOXO1)* and PR-responsive genes (*RORB*, *KLF15)*. Here, our studies provide novel tools to study BMP signaling pathways and highlight the fundamental roles of SMAD1/5 in mediating both BMP signaling pathways and the transcriptional response to progesterone (P4) during early pregnancy.

63 **INTRODUCTION**

64 Infertility is an emerging health issue that affects approximately 15% of couples[1]. One in five women
65 aged 15 to 49 years old with no prior births suffers from infertility in the United States[2]. One important
66 factor affecting fertility is failed embryo implantation or subsequent post-implantation loss due to
67 endometrial defects. This is evident from the high number of failed pregnancies, with as many as 15% of
68 pregnancies resulting in early pregnancy losses[3]. Understanding the molecular mechanism of how the
69 maternal endometrium becomes suitable for embryo implantation and eventual decidualization, will be
70 the key to eradicating global concerns related to infertility and early pregnancy losses.

71 The transforming growth factor β (TGFβ) family plays diverse roles in development, physiology, and
72 pathophysiology[4,5], and in particular, signaling pathways downstream of the bone morphogenetic protein
73 (BMP) subfamily are essential for decidual formation[6,7]. There are more than 30 TGFβ family ligands,
74 and these ligands signal through complexes of transmembrane type 1 Activin-Like Kinases (ALK)
75 receptors (ALK1, ALK2, ALK3, ALK6) and transmembrane type 2 receptors (BMPR2, ACVR2A,
76 ACVR2B) and then phosphorylate downstream SMAD1 and SMAD5 proteins. Phosphorylated SMAD1/5
77 form heteromeric complexes with SMAD4 and translocate to the nucleus to induce specific transcriptional
78 programs. Our laboratory and others have used genetically engineered mouse models with deletions of
79 ligands, receptors, and downstream effectors of BMP signaling pathways to establish that BMP signaling
80 pathways are major regulators of early pregnancy[6-12].

81 A successful pregnancy begins with reciprocal crosstalk between the maternal endometrium and the new
82 blastocyst during the peri-implantation window. Effective implantation requires precise synchronization
83 between the development of the blastocyst and the transformation of the maternal endometrium into a
84 functional decidua. Endometrial stromal fibroblasts undergo the decidualization process in which they
85 differentiate into unique secretory decidual cells that offer a supportive and immune-privileged
86 microenvironment required for embryo implantation and placental development. Decidualizing stromal
87 cells can react to individual embryos in a way that either supports the implantation and subsequent
88 embryonic development or exerts early rejection[13,14]. Aberrant decidualization processes are observed in
89 patients with recurrent pregnancy loss (RPL), displaying a disordered pro-inflammatory response,
90 decreased induction of decidual marker genes, and abnormal responses to embryonic human chorionic
91 gonadotropin[13,15,16]. In addition to affecting early pregnancy outcomes, defective decidualization is also
92 involved in the maternal etiology of preeclampsia, causing abnormal placental phenotype[17,18]. The
93 process of decidualization is tightly regulated by hormone signaling pathways (estrogen, E2, and
94 progesterone, P4), as well as by BMP signaling pathways. Our recent studies found that endometrial
95 *Smad1* deletion had no significant effect on fertility, *Smad5* conditional deletion resulted in subfertility,
96 while double *Smad1/5* conditional deletion led to infertility due to implantation and decidualization
97 defects[9]. The uteri of mice with double conditional *Smad1/5* deletion also displayed decreased response

98 to P4 during the window of implantation, suggesting synergy between the two pathways. However, the
99 mechanistic genomic actions of SMAD1 and/or SMAD5 in the uterus have not been explored, partly
100 because there are no specific antibodies that distinguish phospho-SMAD1 versus phospho-SMAD5.

101 In this study, we define how SMAD1/5 instructs the decidualization process using genomic approaches in
102 newly generated transgenic mouse lines. We inspect the potential crosstalk between P4 and BMP
103 signaling pathways mediated by SMAD1/5. Together, our study demonstrates that SMAD1 and SMAD5
104 exhibit shared and unique genomic binding features and further reveals that SMAD1/5 contributes to the
105 P4 response through transcriptional reprogramming during decidualization.

106 MATERIALS AND METHODS

107 Generation of Knock-in Mouse Lines

108 *Smad5*$^{PA/PA}$ knock-in (KI) mice were generated using a similar approach as previously described[19].
109 Briefly, single-guide RNA (sg-RNA) was designed to target the regions close to the start codon (Figure
110 1A,B) and the sgRNA sequence was inserted into the pX459 V2.0 plasmid (#62988, Addgene). The
111 reference plasmids containing PA tag sequence were constructed in pBluescript II SK (+) vector (Agilent,
112 Palo Alto, CA, USA). One µg of guide RNA inserted vector and 1.0 µg of reference plasmid were co-
113 transfected into EGRG01 embryonic stem (ES) cells. Twelve ES clones out of 48 had the expected
114 knock-in allele. ES cell clones that possessed the proper KI allele were injected into ICR embryos and
115 chimeric blastocysts were transferred into pseudopregnant females. Chimeric male mice were mated
116 with B6D2F1 female mice to obtain the PA-tagged SMAD5 KI heterozygous mice. Homozygous
117 *Smad5*$^{PA/PA}$ mice were maintained in the C57BL/6 J × 129S5/SvEvBrd mixed genetic background. To
118 generate *Smad1*$^{HA/HA}$ mice, Cas9 protein (Thermo Fisher, A36497), sg-RNA, and a repair oligo of
119 homology-directed repair (HDR) containing HA-tag and linker sequences were electroporated into
120 zygotes harvested from *in vitro* fertilization using B6D2F1 male and female mice. An ECM830
121 electroporation system (BTX, Holliston, MA) was used for electroporation. Subsequently, embryos were
122 cultured overnight to the 2-cell stage and then transferred to the oviducts of pseudopregnant CD-1 mice
123 (Center for Comparative Medicine, Baylor College of Medicine). Pups were further screened for
124 successful heterozygous or homozygous knock-in alleles by PCR using primers spanning across the HA
125 tag. Sequences of sgRNA, the single-stranded repair oligo for HDR and primer used for genotype are
126 listed in Supplementary Table 1.

127 Animal ethics compliance and tissue collection

128 All mice were housed under standard conditions of a 12-hour light/dark cycle in a vivarium with controlled
129 ambient temperature (70˚F ± 2˚F and 20-70% relative humidity). All mouse handling and experimental
130 procedures were performed under protocols approved by the Institutional Animal Care and Use

131 Committee of Baylor College of Medicine. All experiments were performed with female mice aged
132 between 7 to 12 weeks with a C57BL/6 J × 129S5/SvEvBrd mixed genetic background. All mice were
133 euthanized using isoflurane induction followed by cervical dislocation, and tissues were snap-frozen in
134 liquid nitrogen.

135 **Cleavage Under Targets and Release Using Nuclease (CUT&RUN) Approach**

136 Nuclei from uterine tissues were purified following a previously published protocol[20]. The experiments
137 were performed using pooled biological replicates from two mice that were processed as technical
138 replicates throughout the CUT&RUN procedure and analysis. In short, uteri were harvested from
139 pregnant mice at 4.5 days post coitus and washed with cold swelling buffer (10 mM Tris-HCl pH 7.5,
140 2 mM $MgCl_2$, 3 mM $CaCl_2$, 1X Protease Inhibitor Cocktail (PIC, Roche, 11836170001)) immediately after
141 collection. Then tissue was cut into small pieces (~2-3mm) using scissors, while submerged in cold
142 swelling buffer. Nuclear extract was prepared by dounce homogenization in cold swelling buffer (using a
143 size 7 dounce) and filtered using the cell strainer (100 µm, BD Biosciences). Lysate was centrifuged at
144 400 g for 10 min, then resuspended in lysis buffer (swelling buffer with 10% glycerol and 1% CA-630, 1X
145 PIC) using end-cut or wide-bore tips and incubated on ice for 5 min. Nuclei were washed twice with lysis
146 buffer and resuspended in lysis buffer. Next, CUT&RUN procedure largely follows a previous protocol[21].
147 Briefly, around 500,000 nuclei were used per reaction. 10 µl of concanavalin-coated beads (Bangs Labs,
148 BP531) were washed twice in Bead Activation Buffer (20 mM HEPES, pH 7.9, 10 mM KCl, 1 mM $CaCl_2$,
149 1 mM $MnCl_2$) for each reaction. Then, beads were added to nuclei resuspension and incubated for 10
150 mins at room temperature. After incubation, bead-nuclei complexes were resuspended in 100 µl
151 Antibody Buffer (20 mM HEPES, pH 7.5, 150 mM NaCl, 0.5 mM Spermidine, 1X PIC, 0.01% digitonin,
152 and 2mM EDTA) per reaction. One µg of IgG antibody (Sigma, I5006), HA antibody (EpiCypher, 13-
153 2010), PA antibody (Fuji Film, NZ-1) and PR antibody (Cell Signaling, D8Q2J) were added to each group
154 respectively. After overnight incubation at 4 °C, bead-nuclei complexes were washed twice with 200 µl
155 cold Dig-Wash buffer (20 mM HEPES pH=7.5, 150 mM NaCl, 0.5 mM Spermidine, 1X PIC, 0.01%
156 digitonin) and resuspended in 50 µl cold Dig-Wash buffer with 1 µl pAG-MNase (EpiCypher, 15-1016)
157 per reaction. After incubation at room temperature for 10 min, bead-nuclei complexes were washed twice
158 with 200 µl cold Dig-Wash buffer and resuspended in 50 µl cold Dig-Wash buffer, then 1 µl 100 mM
159 $CaCl_2$ was added to each reaction. The mixture was incubated at 4 °C for 2 hours and the reaction was
160 stopped by adding 50 µl Stop Buffer (340mM NaCl, 20 mM EDTA, 4 mM EGTA, 0.05% Digitonin, 100
161 ug/mL RNase A, 50 mg/mL glycogen, 0.5 ng E. coli DNA Spike-in (EpiCypher, 18-1401)) and incubate at
162 37 °C for 10 min. The supernatant was collected and subjected to DNA purification with phenol-
163 chloroform and ethanol precipitation. Sequencing libraries were prepared using NEBNext Ultra II DNA
164 Library Prep Kit (New England BioLabs, E7645) following manufacture's protocol. Paired-end 150 bp
165 sequencing was performed on a NEXTSeq550 (Illumina) platform.

166 **Bioinformatic Analysis for CUT&RUN data and re-analysis of published single-cell RNA seq data**

167 For CUT&Run data, raw data were de-multiplexed by bcl2fastq v2.20 with fastqc for quality control.
168 Clean reads were mapped to reference genome mm10 by Bowtie2, with parameters of --end-to-end --
169 very-sensitive --no-mixed --no-discordant --phred33 -I 10 -X 700. For Spike-in mapping, reads were
170 mapped to E. coli genome U00096.3. Duplicated reads were removed, and only uniquely mapped reads
171 were kept. Spike-in normalization was achieved through multiply primary genome coverage by scale
172 factor (100000 / fragments mapped to E. coli genome). CUT&RUN peaks were called by SECAR[22] with
173 the parameters of -norm -stringent -output. Track visualization was done by bedGraphToBigWig[23], bigwig
174 files were imported to Integrative Genomics Viewer for visualization. For peak annotation, common
175 peaks were identified with 'mergePeaks' function in HOMER v4.11[24] and then genomic annotation was
176 added by ChIPseeker [25]. Motif analysis was conducted through HOMER v4.11 with parameter set as
177 findMotifsGenome.pl mm10 -size 200 -mask[24]. Peak heatmaps were plotted using deepTools 2.4.2 with
178 clustering options set to k-means[26]. For imputing the cell fractions using published mouse uterine bulk
179 and single-cell RNA seq data, single-cell RNA-seq with cell type reference from 5.5 dpc mouse uterus
180 was derived from GSE226417, bulk RNA-seq of the 3.5 dpc mouse uterus was derived from
181 GSE152675. Signature matrix and cell fraction profiles were conducted through CIBERSORTx[27]. Briefly,
182 reference gene expression signature matrix was generated by “Create Signature Matrix” module with
183 default settings. Next, cell fractions were calculated using “Impute Cell fractions” module in the absolute
184 mode, which scales each annotated cellular fractions to an absolute value that reflects its absolute
185 proportion in the bulk sample. For human single-cell RNA seq data, raw data was obtained from EMBL-
186 EBI under accession No. E-MTAB-10287. Cells with low coverage (less than 500 genes detected) were
187 filtered, then gene counts were normalized for each cell by converting counts to quantiles and obtaining
188 the corresponding values from a normal distribution. Then normalized cell vectors are concatenated
189 along the gene panel. Plot visualization was conducted through CELLXGENE platform.[28]

190 **Western Blot Analysis of Immunoprecipitation (IP-WB)**

191 Tissues were pulverized in liquid nitrogen and then lysed using NETN buffer (20 mM Tris-HCl, pH 8.0,
192 150 mM NaCl, 0.5 mM EDTA, 10% Glycerol, and 0.5% NP-40). Protein concentration was determined by
193 BCA Protein Assay Kit (Thermo Fisher, 23225). 1.5 mg of total protein lysate was used for IP. IP was
194 performed by adding HA antibody (Cell Signaling, C29F4) or PA antibody (Fuji Film, NZ-1) to the lysate
195 and incubate for 1 hour at 4 °C. Subsequently, protein G magnetic beads (Thermo Fisher, 88847) were
196 added for an additional 1 hour at 4 °C. Then, the beads were washed five times with NETN buffer, and
197 denatured in sample buffer (Thermo Fisher, NP0007) for further analysis by Western blot. For western
198 blot procedures, briefly, denatured protein lysates were run on the 4 to 12%, Bis-Tris protein gels
199 (Thermo Fisher, NP0321BOX) followed by electrophoretic transfer to nitrocellulose membrane. The

200 membrane then went through blocking by 5% milk in Tris-buffered saline with Tween20 (TBST), followed
201 by incubation overnight at 4 °C in the primary antibodies anti-HA (Cell Signaling, C29F4), anti-PA (Fuji
202 Film, NZ-1), anti-SMAD1 (Life technologies, 385400) and anti-SMAD5 (ProteinTech, 12167-1-AP) at
203 1:1,000 dilution. The next day, membranes were washed three times with TBST, then incubated with
204 horseradish peroxidase–conjugated secondary antibody for 1 h at room temperature, then washed three
205 times with TBST, developed and imaged on iBright Imaging System (FL1500).

206 **Primary endometrial stromal cells isolation/RNAi/decidualization**

207 Studies using human specimens were conducted as indicated in a protocol approved by the Institutional
208 Review Board at Baylor College of Medicine, H-51900. Human endometrial stromal cells were collected
209 from healthy volunteers' menstrual effluent as previously reported[29-31]. (N=3) In brief, samples were
210 collected by participants in a DIVA cup during the 4-8 hours on the first night of menses and stored in
211 DMEM/F12 with 10% FBS, antibiotic/antimycotic and 100μg/ml Primocin in a cold insulated pack until
212 processing in the laboratory on the day of collection. The effluent was digested with 5 mg/ml collagenase
213 and 0.2 mg/ml DNase I for 20 min at 37 °C, then the cell pellet was collected by centrifuging at 2,500 rpm
214 for 5 min at room temperature. Next, red blood cell lysis was performed by resuspending the cell pellet in
215 20 ml of 0.2% NaCl for 20 seconds and neutralized with 20 ml of 1.6% NaCl. Then the solution was then
216 centrifuged at 2,500 rpm for 5 min. Five ml complete medium (DMEM/F12 supplement with 10% FBS, 1X
217 Antibiotic-Antimycotic + 100 μg/ml Primocin) was used to resuspend the pellet and the solution was
218 passed through 100 μm and 20 μm cell strainer sequentially. The flowthrough containing the stromal
219 cells was centrifuged for 5 min at 2,500 rpm and the pellet was resuspended in 10 ml complete medium
220 and plated in a 10 cm dish. siRNA knockdown was performed using Lipofectamine RNAiMAX following
221 the manufacturer's protocol. In brief, 0.2 million stromal cells were plated in a 12-well plate one day
222 before transfection. On the day of transfection, 2 μl siRNA (20 μM, Dharmacon, D-001810-10, L-012723-
223 00-0005, L-015791-00-0005) and 3 μl Lipofectamine RNAiMAX were diluted in 50 μl Opti-MEM
224 respectively and then mixed to incubate at room temperature for 15 min. Then, the complex was added
225 dropwise onto the cells. 24 h after transfection, medium was changed to DMEM/F12 supplement with 2%
226 charcoal stripped FBS. Decidualization was induced by the addition of 35 nM estradiol (Sigma, E1024), 1
227 μM medroxyprogesterone (Sigma, 1378001), and 0.05 mM cyclic adenosine monophosphate (Axxora,
228 JBS-NU-1502L) for 4 days with media changes every 48 hours.

229 **RNA Extraction and RT-qPCR**

230 For mRNA extraction from stromal cells, cells were lysed with TRIzol and processed using the DirectZol
231 kit (Zymo, R2051) following manufacturer's procedures. Approximately 100 ng of mRNA was reverse
232 transcribed into cDNA using iScript cDNA Supermix (Bio-Rad, 1708890) and amplified using specific
233 primers listed in Supplementary Table 1. Primers were amplified using 2X SYBR Green Reagent (Life

234 Technologies, 4364346) using a BioRad CFX384 Touch Real Time PCR Detection System. Data
235 analysis was performed by calculating ΔΔCT value towards the geometric mean of *GAPDH, ACTB* and
236 *RPL13A* and then normalized to siCTL. P-value was determined by One-Way ANOVA test with post hoc
237 Tukey test using GraphPad Prism. * $P \leq 0.05$, ** $P \leq 0.01$, *** $P \leq 0.001$, **** $P \leq 0.0001$.

238

239 **RESULTS**

240

241 **Generation of Mouse Models with Global HA-Tagged SMAD1 and PA-Tagged SMAD5 Proteins**

242 Activation of BMP signaling pathways has been established as one of the hallmarks of the
243 decidualization process[32,33]. Canonically, SMAD1/5 are regarded as downstream effectors of BMP2
244 signaling pathways to regulate decidual-specific gene expressions[6,34]. However, our recent findings
245 demonstrated that SMAD1/5 can also affect the sensitivity of the endometrium towards E2 and P4
246 stimulation[9]. Since we observed phenotypical differences between uterine-specific single SMAD1 and
247 single SMAD5 deletion mice, it is beneficial to delineate the role of SMAD1 and SMAD5 in mediating P4
248 responses during early pregnancy. We used CRISPR technology to generate genetically engineered
249 knock-in mice with an HA-tagged *Smad1* allele (herein called *Smad1*$^{HA/HA}$) and PA-tagged *Smad5* allele
250 (herein called *Smad5*$^{PA/PA}$) as shown in Figure 1A, B. The HA tag and the PA tag were inserted into the
251 N-terminus of the SMAD1 and SMAD5 proteins, respectively. Sanger sequencing was used to confirm
252 genomic insertion (Figure 1A, B). To validate the global detection of tagged proteins, we performed
253 immunoprecipitation followed by western blot analysis on different tissues from *Smad1*$^{HA/HA}$ and
254 *Smad5*$^{PA/PA}$ mice. We confirmed the HA and PA antibodies can readily detect HA-tagged SMAD1 and
255 PA-tagged SMAD5 proteins at the predicted size (Figure 1C, D). We also demonstrated the molecular
256 size and expression pattern of HA antibody detected SMAD1 protein was comparable to the SMAD1
257 antibody detected SMAD1 protein across different tissue types. Similarly, PA antibody showed
258 comparable signal intensity to the SMAD5 antibody in detecting SMAD5 protein across different tissue
259 types (Figure 1C, D). Thus, we successfully generated viable mouse models with global HA-tagged
260 SMAD1 and PA-tagged SMAD5 proteins.

261 **SMAD1 and SMAD5 Exhibit Shared and Unique Genomic Binding Sites During Decidualization**

262 The BMP signaling pathway regulates multiple key events during early pregnancy[5], mediated through
263 receptor-regulated SMAD proteins, including SMAD1 and SMAD5. As transducers of the BMP signaling
264 pathway, phosphorylated SMAD1 and SMAD5 form homomeric complexes and then couple with SMAD4
265 to assemble hetero-oligomeric complexes in the nucleus to execute transcription programs. Our previous
266 studies revealed that conditional ablation of SMAD1 and SMAD5 in the uterus decreased P4 response
267 during the peri-implantation period, suggesting that the transcriptional activities of PR depend on

268 BMP/SMAD1/5 signaling[9]. Furthermore, previous genome-wide PR binding studies show that SMAD1
269 and SMAD4 binding motifs are enriched in PR binding sites in the uterus[35].

270 To determine the shared and unique transcriptional regulomes of SMAD1 and SMAD5 contributing to the
271 diverse effects of BMP and P4 signaling pathways during decidualization, we first utilized Cleavage
272 Under Targets & Release Using Nuclease (CUT&RUN)[21] coupled with next generation sequencing to
273 profile genomic loci bound by SMAD1, SMAD5 and PR from mouse uterine tissues. We performed
274 CUT&RUN on the uterine tissues collected at 4.5 days post coitus (dpc), the time when the fertilized
275 embryo reaches the uterus physically and initiates the decidualization program[36] (Figure 2A). After
276 aligning CUT&RUN reads to the mm10 mouse genome, we called peaks using Sparse Enrichment
277 Analysis for CUT&RUN (SEACR)[22]. To identify high confidence peaks, background noise was
278 normalized to IgG and the stringent criteria for peak calling in SEACR was used. After merging common
279 peaks from two biological replicates, we identified 118,778 peaks for SMAD1 and 166,025 total peaks for
280 SMAD5. We visualized the enrichment of SMAD1 and SMAD5 peaks to the overall aligned chromatin
281 regions with clustering for preferential enrichment, as shown in Figure 2B. Peaks in cluster 1 exhibit a
282 shared enrichment for both SMAD1 and SMAD5, whereas clusters 2 and 3 demonstrate preferential
283 enrichment for SMAD5 and SMAD1, respectively. We found that 7.55% of SMAD1 peaks and 9.53% of
284 SMAD5 peaks were located within the ± 3 kb of the promoter regions (Figure 2C, D). This corresponded
285 to 10,368 genes that were directly bound by SMAD1 at the promoter regions (± 3 kb), whereas 18,270
286 genes were directly bound by SMAD5 at the promoter regions (± 3 kb). Among these, 4,933 genes were
287 found in common between SMAD1 (47.5%) and SMAD5 (27.0%), while 2,744 and 7,427 genes were
288 found to be uniquely bound by SMAD1 and SMAD5, respectively, providing evidence for the shared and
289 unique functions of SMAD1 and SMAD5 at the transcriptional level (Supplement Figure 1A). Hence,
290 interpreting how the binding events correlate to biological activity requires comparisons with gene
291 expression profiling in a tissue-specific manner.

292

293 **Identification of Direct Target Genes of SMAD1 and SMAD5 During Early Pregnancy**

294 To pinpoint the direct target genes of SMAD1 and SMAD5, we integrated transcriptomic data from
295 previously published[9] SMAD1/5 double conditional knockout mice using progesterone receptor cre
296 (SMAD1/5 cKO) (GSE152675) with SMAD1 and SMAD5 genomic data from this paper. We cross-
297 compared the differentially expressed genes in the transcriptomic data to the SMAD1 and SMAD5 bound
298 genes, respectively. Among the 805 significantly up-regulated genes, we identified 449 genes that were
299 both significantly up-regulated upon SMAD1/5 depletion and were directly bound by SMAD1 and
300 SMAD5, whereas 187 of the up-regulated genes were bound by SMAD5 only and 30 were bound only by
301 SMAD1 (Figure 3A). Among the 683 significantly down-regulated genes, we identified 523 genes that

302 were both significantly down-regulated upon SMAD1/5 depletion and were directly bound by SMAD1 and
303 SMAD5, whereas 83 of the down-regulated genes were bound by SMAD5 only and 13 were bound by
304 SMAD1 only (Figure 3B, Supplementary Table 2).

305 Next, we utilized Binding and Expression Target Analysis (BETA) algorithm[37] to perform motif enrichment
306 analysis of the direct target genes to identify putative co-factors working together with SMAD1 and
307 SMAD5 in controlling gene expression (Figure 3C,D, Supplement Files1,2). "Up-targets" represent genes
308 that were up-regulated in the SMAD1/5 cKO mouse uteri and showed either a SMAD1 or a SMAD5
309 binding site in the genomic profiling data. Similarly, "down-targets" represent genes that were down-
310 regulated in the SMAD1/5 cKO mouse uteri and displayed either a SMAD1 or a SMAD5 binding site.
311 Thus, motifs enriched in the "up-targets" indicate potential repressive SMAD1/5 co-factors while motifs
312 enriched in the "down-targets" indicate potential SMAD1/5 co-activators. Among the "up-targets" of
313 SMAD1, MYB Proto-Oncogene (*Myb*)/MYB Proto-Oncogene Like 1(*Mybl1*) motif was the most highly
314 enriched with a P-value of 1.85E-02. *Myb* and *Mybl1* transcription factors belong to MYB gene family,
315 which has been well-defined in controlling cell survival, proliferation and differentiation in cancer[38]. In
316 addition, they have also been reported to be E2 induced in human uterine leiomyoma samples[39].
317 Homeobox containing 1 (*Hmbox1*) and Krüppel-like factor (*Klf*) family members (*Klf4/Klf1/Klf12*) were
318 also identified as potential repressive co-factors of SMAD1 with P-values of 2.85E-02 and 3.75E-02
319 respectively (Figure 3C). Of note, *KLF4* has been reported to inhibit the binding activity of estrogen
320 receptor α (ERα) to estrogen response elements in promoter regions[40]. Among the "up-targets" of
321 SMAD5, EBF Transcription Factor 1 (*Ebf1*) motif was the most enriched with a P-Value of 1.57E-02.
322 Interestingly, *Ebf1* can directly repress the transcription of Forkhead box protein O1 (*Foxo1*)[41]. It is also
323 recognized as downstream effector of steroid hormone receptors in the mouse uterus[42]. Additionally,
324 motifs from transcription factors *Zfp128* and *Otx1* were also significantly enriched in the up-regulated
325 genes bound by SMAD5 (Figure 3D). Taken together, our enrichment analysis provided robust evidence
326 for identifying novel co-factors of SMAD1/5, and such co-regulating mechanisms are in line with the
327 unopposed E2 response observed in the SMAD1/5 cKO mice[9]. Furthermore, odd-skipped–related genes
328 (*Osr1* and *Osr2*) were identified as potential co-activators for SMAD1. *Osr2* has been reported to be
329 highly expressed in the human endometrium[43], and it was also abundantly detected at the protein level in
330 the human decidual tissues[44]. Decreased OSR2 level was observed in the patients with recurrent
331 spontaneous abortion and knockdown of *OSR2* impairs the decidualization process in the human
332 endometrial stromal cells[44]. Moreover, OSR1 has been reported to suppress BMP4 expression, which in
333 turn reduced the Wnt/β-catenin signaling pathways during lung development in xenopus[45]. Apart from
334 Osr family, motifs in the Homeobox genes (HOX) were found to be enriched in the "down-targets" from
335 both SMAD1 and SMAD5 datasets. Specifically, *Hoxa11/Hoxd12/Hoxc10* were predicted to be co-
336 activators for SMAD1 while *Hoxd10* was indicated to be closely interacting with SMAD5. Indeed, HOX

genes are critical for endometrial development in normal and disease conditions and are essential during the establishment of pregnancy[46-49].

With direct target genes of SMAD1 and SMAD5 identified, we then analyzed the Gene Ontology enrichment for the SMAD1/5 shared up-targets and down-targets, respectively. We found that “up-targets” genes exhibit enrichment for regulation of cell-cell adhesion, cell junction organization and desmosomes organization (Figure 3E, Supplementary Table 3). Moreover, among the “down-targets” genes, we found the enrichment for blood vessel / vasculature development and extracellular matrix organization categories (Figure 3F, Supplementary Table 4). Indeed, during early pregnancy, the stimulation from corpus-luteum derived P4 enabled the endometrium to be transformed to a receptive state, which allows subsequent embryo attachment and develop through the epithelium into the stromal sections[32]. During this process, apportioned direct cell-cell contacts are ensured by tight and adherent junctions and such interactions are key in facilitating implantation and embryo invasion. In accordance with our findings, desmosomes and adherens junctions were extensively described to decline in the early pregnancy period, which facilitates the invasion of trophoblast through the epithelial layer[50-53]. In addition, the stromal compartment of the endometrium also undergoes profound vascular remodeling. Precise regulations of angiogenesis are required to establish an extensive vascular network, which is essential to ensure blood supply and successful embryonic development[54,55]. Collectively, our findings present evidence that emphasizes the shared roles of SMAD1 and SMAD5 in facilitating endometrial transitions during early pregnancy.

Direct Target Genes of SMAD1 and SMAD5 Maintain the Homeostasis of Uterine Function

To discover novel direct target genes of SMAD1/5, we visualized key genes of interest from the up-targets and down-targets. As shown in Figure 4A, data from RNA-seq represents the decrease of several "down-targets” in the SMAD1/5 cKO mouse uteri, including Retinoic Acid-Related Orphan Receptor B (*Rorb*), Follistatin (*Fst*), Lymphoid Enhancer Binding Factor 1 (*Lef1*), and Insulin Like Growth Factor 1 (*Igf1*). Integrative Genomics Viewer (IGV) track view shows the exemplary SMAD1/5 binding activities near the promoter regions of *Rorb* and *Fst* Figure 4B, demonstrating that these genes are bona fide direct target genes of SMAD1/5. *Rorb* belongs to the nuclear receptor families in the retinoic acid (RA) signaling pathways[56] and is considered as a marker for mesenchymal progenitor cells in the stroma compartment of the endometrium[57]. In murine models, deficient RA signaling through the perturbation of RA receptor in the uterus leads to implantation and decidualization failure[58]. *Fst* binds several TGFβ family ligands and thereby inhibits TGFβ family signaling extracellularly[59]. Under physiological conditions, *Fst* is up-regulated in the decidua during early pregnancy. Conditional deletion of *Fst* in the mouse uterus results in severe subfertility with a phenotype of non-receptive epithelium and poorly-differentiated stroma[60]. Notably, RA signaling deficiency also decreases *Fst* levels in the uterus and systematic

371 administration of FST can fully rescue the deficient-decidualization phenotype but not the non-receptive
372 phenotype observed in the RA receptor mutant mice[58]. Our results suggest a direct relationship between
373 BMP and RA signaling pathway, accomplished by SMAD1/5 at the transcriptional level, likely
374 establishing a positive signaling feedback loop. Apart from being a crucial transcriptional activator,
375 SMAD1/5 also plays a role in repressing key gene expression pathways. Shown in Figure 4C, upon the
376 deletion of SMAD1/5 in the mouse uteri, several E2-responsive genes were significantly up-regulated,
377 including Fibroblast Growth Factor Receptor 2 (*Fgfr2*), Matrix Metallopeptidase 7 (*Mmp7*) and Wnt
378 Family Member 7B (*Wnt7b*). In addition, *Inhbb*, a downstream target of *Fst*[60], is also a target gene of
379 SMAD1/5 that resulted in transcriptional repression. SMAD1/5 binding on the *Fgfr2* and *Mmp7* genes are
380 exemplified in an IGV track view in Figure 4D. *Fgfr2* and its ligands regulate epithelial cell proliferation
381 and differentiation. Components of the Fibroblast Growth Factor (*Fgf*) signaling pathway are cyclically
382 expressed in the uterus and act as paracrine and/or autocrine mediators of epithelial-stromal
383 interactions[61,62]. During early pregnancy in mice, P4 inhibits expression of *Fgf2* in the stromal cells, which
384 is critical to counteract the E2-driven epithelial proliferation[61]. Similar observations are reported in gilts,
385 where the expression of *Fgfr2* decreased alongside with increased parity of the sows[63]. It is also
386 noteworthy that loss of function of *Fgfr2* in the mouse uterus leads to luminal epithelial stratification and
387 peri-implantation pregnancy loss[62]. Moreover, *Mmp7* and *Wnt7b* are up-regulated upon E2 stimulation
388 and participate in the re-epithelialization of the endometrium and implantation process, respectively[64-66].
389 In accordance with the phenotype of hyperproliferative endometrial epithelium during early pregnancy
390 observed SMAD1/5 cKO mice, we demonstrated that the suppression of key E2-responsive genes, such
391 as *Fgfr2* and *Mmp7,* by SMAD1/5 maintains the precise balance between E2 and P4.

392 To explore the major cell types regulated by SMAD1/5, first, we used CIBERSORTx[27] to analyze and
393 depict changes in the cell populations upon SMAD1/5 depletion in the mouse uterus during early
394 pregnancy. By imputing the bulk uterine gene expression profiles to previously published mouse uterine
395 single-cell datasets[67] using CIBERSORTx[27], we were able to compare changes across both samples and
396 cell types upon the SMAD1/5 perturbation in the mouse uterus. We highlight the proportional increase in
397 the epithelial cells, as well as the decrease in the decidual stromal cells and smooth muscle cells in mice
398 lacking uterine SMAD1/5 during the peri-implantation phase (Supplement Figure 1B). Such cell
399 populational changes are in line with the phenotypical observations of decidualization failure and
400 excessive proliferation in the epithelial compartment. In addition, to explore the expression patterns of
401 SMAD1/5 direct targets in human, we profiled the expression levels of the key “up-targets” and “down-
402 targets” in the different cell types of the human endometrium. Using previously published single-cell RNA
403 seq data of human endometrium[68], we visualized the expression patterns of suppressive targets and
404 activating targets of SMAD1/5 (Figure 4E). Apart from the major epithelial and stromal compartments,
405 SMAD1/5 target genes are also widely expressed in the immune cell populations. Such observations

406 reinforced the importance of the BMP signaling pathways in establishing an immune-privileged
407 environment at the maternal-fetal interface[69].

408 **SMAD1 and SMAD5 Co-regulate PR Target Genes**

409 SMAD1/5 cKO mice were infertile due to endometrial defects and displayed decreased P4 response
410 during the peri-implantation period[9]. Hence, we hypothesized that SMAD1 and SMAD5 act as co-
411 regulators of P4-responsive genes during the window of implantation and are required for endometrial
412 receptivity and decidualization. By determining the genomic co-occupancy of SMAD1, SMAD5 and PR,
413 we aimed to clarify the transcriptional interplay between the BMP and P4 signaling pathways. To this
414 end, we performed additional PR CUT&RUN experiments on the uteri of mice collected at 4.5 dpc and
415 identified 134,737 peaks showing PR binding activities (Figure 5A). Based on the k-means clustering
416 results of the peaks, we demonstrated clusters with shared occupancy between SMAD1/5 and PR
417 (cluster 1), preferential deposition in the SMAD1 (cluster 2), SMAD5 (cluster 4) and PR (clusters 3,5),
418 respectively. Interestingly, between clusters 3 and 5, although the primary enrichment is for PR, overall
419 the signal intensities for SMAD5 are higher in cluster 5. Together with previous analysis on genes
420 uniquely or commonly bound by SMAD1/5 (Supplement Figure 1A), we speculate such observation can
421 be attributed to a subset of the genes that are potentially co-regulated by SMAD5 and PR. From the
422 gene perspective, we identified 7,393 genes that were directly bound by PR at the promoter regions (± 3
423 kb), among which, 2596 genes were also concurrently bound by both SMAD1 and SMAD5 at the
424 promoter regions (± 3 kb) (Supplement Figure 1C).

425 Next, we performed KEGG pathway enrichment for the genes co-bound by SMAD1, SMAD5 and PR. As
426 expected, pathways critical for decidualization such as relaxin signaling pathways and WNT signaling
427 cascade were identified in the enrichment results (Figure 5B, Supplementary Table 5). We visualized
428 exemplary genes co-regulated by SMAD1, SMAD5 and PR and presented in the normalized IGV track
429 view (Figure 5C). We demonstrated SMAD1, SMAD5 and PR showed co-occupancy at the loci of the
430 SRY-Box Transcription Factor 17 (*Sox17*), Inhibitor of DNA binding 2 (*Id2*), Forkhead box protein O1
431 (*Foxo1*), Insulin-like growth factor 1 (*Igf1*), Transforming growth factor beta receptor 2 (*Tgfbr2*) and
432 RUNX family transcription factor 1 (*Runx1*) (Figure 5C). *Sox17* has been reported as one of the direct
433 target genes of PR[35] and is essential for uterine functions during implantation and early pregnancy[70,71].
434 More recent studies also showed the importance of *Sox17* in regulating uterine epithelial–stromal
435 crosstalk and its indispensable role in female fertility[72]. We provided evidence that *Sox17* is also directly
436 regulated by SMAD1/5 complexes. Our results indicated that *Id2*, considered as canonical direct
437 transcriptional targets of BMP-SMAD signaling[73,74] is also regulated by PR. We also confirmed that
438 known P4-responsive genes such as *Tgfbr2*[75] and *Runx1*[76], as well as decidual markers such as *Foxo1*[77]
439 and *Igf1*[78], were co-regulated by SMAD1, SMAD5 and PR (Figure 5C).

440 To identify additional transcription factors that are associated with the regulatory interplay between
441 SMAD1/5 and PR during decidualization, we performed unbiased motif analysis on the shared
442 CUT&RUN peaks between SMAD1/5 and PR. We reported the top 10 transcription factors harboring the
443 enriched motifs, including NANOG, Homeobox A protein family (HOXA11 and HOXA9), NK6 homeobox
444 1(NKX6.1), TGFB induced factor homeobox 2 (TGIF2), FOS, RUNX family transcription factor 2
445 (RUNX2), Androgen receptor (AR), SOX17 and Lymphoid enhancer-binding factor 1 (LEF1) (Figure 5D,
446 Supplementary Table 6). Many of these putative interactors have been reported to interact with the
447 SMAD proteins in other biological processes. For example, NANOG interacts with SMAD1 during
448 mesoderm differentiation[79]. HOXA9 forms heterodimers with SMAD4, leading to BMP-driven initiation of
449 transcription from the mouse *Opn* promoter *in vitro*[80,81]. Transcription factor AP-1 family (FOS) and
450 RUNX2, as well as β-catenin/Lef1 complex, increase the effectiveness and specificity of DNA binding
451 activities of SMAD1/5 in response to BMP ligand stimuli[82-84]. To further evaluate the key roles of
452 SMAD1/5 as major uterine transcription regulators, we cross-compared the genomic binding sites of
453 SMAD1/5 with known key transcription factors, namely aforementioned SOX17 (Supplement Figure 1F,
454 Supplementary Table 7), as well as NR2F2 (Supplement Figure 1G, Supplementary Table 8), an
455 essential regulator of hormonal response[85], using our CUT&RUN data sets and published mouse uterine
456 SOX17 and NR2F2 ChIP-seq data sets (GSE118328, GSE232583). Among the annotated genes, 5402
457 genes are shared between SMAD1/5 and SOX17, and 1922 genes are shared between SMAD1/5 and
458 NR2F2. Such observations indicate a potential co-regulatory mechanism between SMAD1/5 and other
459 key uterine transcription factors in maintaining appropriate uterine functions. Overall, our analyses
460 demonstrate that the transcriptional activity of SMAD1, SMAD5, and PR coordinate the expression of key
461 genes required for endometrial receptivity and decidualization.

462 **Decidualization of Human Endometrial Stromal Cells Requires SMAD1/SMAD5**

463 We next sought to functionally characterize the role of SMAD1/5 during decidualization in human
464 endometrial stromal cells. To do so, we examined the effect of SMAD1/5 perturbations on the
465 decidualization of primary human endometrial stromal cells (EnSCs). EnSCs were transfected with short
466 interfering RNAs (siRNAs) targeting each gene (*SMAD1* and *SMAD5)* and subjected to *in vitro*
467 decidualization by treatment with E2-cAMP-and MPA (EPC) for 4.5 days (Figure 6A). We hypothesized
468 that the combined SMAD1/5 knockdown would impair the decidualization process significantly compared
469 to cells treated with non-targeting siRNAs. Our results demonstrated that SMAD1/5 knockdown affected
470 decidualization and led to significantly decreased expression of the canonical decidual markers, *PRL and*
471 *IGFBP1* in EnSCs (Figure 6B). The PR co-regulator, *FOXO1*[86]*,* also exhibited a significant decreasing
472 trend in the siSMAD1/5 group. We also examined the expression level of the RA pathway regulator gene,
473 *RORB*, and of the SMAD4-PR target gene, *KLF15*[12], following SMAD1/5 perturbation. We observed a

474 significant decrease in both *RORB* and *KLF15* expression upon SMAD1/5 knockdown during *in vitro*
475 decidualization treatment (Figure 6C). Taken together, our findings indicate SMAD1/5 can modulate PR
476 activity during decidualization and that this transcriptional cooperation is required for the *in vitro*
477 decidualization of primary human endometrial stromal cells.

478 **DISCUSSION**

479 SMAD proteins are canonical transcription factors that are activated in response to TGFβ family signaling
480 and mediate the biological effects of these pathophysiologically critical ligands[83]. While SMAD2 and
481 SMAD3 are downstream of TGFβs, activins, and multiple other family ligands, SMAD1 and SMAD5
482 preferentially transduce BMP signaling pathways and are regarded as pivotal activators for many
483 physiological processes, including bone development, cardiac conduction system development, and
484 embryonic pattern specification[87-89]. Importantly, SMAD1 and SMAD5 are implicated in diverse female
485 reproductive physiology and pathophysiology processes[5,9,90-92].

486 Due to high structural similarity, SMAD1/5 have been suggested to be redundant from the studies in
487 ovarian biology and chondrogenesis[91,93]. However, other studies clearly demonstrated that SMAD1/5
488 have different roles in governing hematopoiesis and uterine functions[9,94]. The DNA binding activities of
489 SMAD1 and SMAD5 have not been readily distinguished from each other due to anti-phospho antibody
490 limitations. To robustly define the roles of SMAD1/5 in regulating transcriptional programs *in vivo*, we
491 produced two genetically engineered mouse models with global knock-in of an HA tag and a PA tag in
492 the *Smad1* and *Smad5* loci, respectively. We showed that SMAD1 and SMAD5 not only have shared
493 transcriptional activities but also have unique roles in uterine physiology. In agreement with previous
494 studies showing that SMAD1/5 function is partially redundant[91,93], we confirmed that SMAD1/5 share a
495 total of 972 direct target genes in the uterus. Furthermore, we demonstrated that 43 genes were uniquely
496 regulated by SMAD1 whereas 270 genes are specifically regulated by SMAD5 only. Our motif analysis
497 also revealed distinct potential co-factors between SMAD1 and SMAD5, providing evidence at the
498 molecular level to mechanistically delineating the distinct roles of SMAD1 and SMAD5 in directing
499 cellular processes in the uterus.

500 Apart from directly regulating target gene expression, our data demonstrate that SMAD1/5 present as
501 dense genomic occupancies. To date, only a limited amount of transcription factors have been
502 investigated using the CUT&RUN-seq technique from the tissue samples due to antibody compatibility
503 issue. We recognize that the binding sites and gene number identified here are quite high; however, the
504 high density of binding events was also observed in the ENCODE[95] chromatin immunoprecipitation
505 followed by sequencing (ChIP-seq) data for SMAD1 and SMAD5 in the human K562 cells, detecting an
506 average of 63,563 peaks for SMAD1 and 109,682 peaks for SMAD5. (Data accessed through GSE95876

507 and GSE127365 from Gene Expression Omnibus). Multiple aspects can contribute to the observation of
508 dense SMAD1/5 genome occupancies. First, transcription factors (TFs) tend to dwell or "search and
509 bind" throughout the genome[96]. Such events may not yield actual biological effects but rather are due to
510 differences in motif binding affinities[97]. Second, apart from robust binding activities, TFs may not initiate
511 transcription programs owing to the lack of co-factors or favorable conditions to exert their functions[98].
512 Additionally, TF binding sites and target genes are unlikely to have a one-to-one relationship. TFs could
513 be positioned from the proximal promoter regions to hundreds of kilobases afar to modulate gene
514 expression. In the meantime, the same binding site could regulate multiple genes by interacting with
515 different promoters in different subpopulations of cells. Lastly, TFs usually direct target gene expression
516 in a cell-type specific manner[99]. Our genomic profiling samples were collected from whole uterus at the
517 time of 4.5 dpc, containing a great range of cell populations, including but not limited to the epithelium
518 (luminal and glandular), stroma (progenitors and differentiated cells), myometrium, endothelium, and
519 immune cell populations. The data is therefore expected to depict the dynamic and complex activities of
520 SMAD1/5 in the entire uterus. Together, the stringent filtering and normalization criteria, comparable
521 peak number to the published dataset and IGV track view visualization collectively validate our
522 CUT&RUN experiments and uncover the enriched regions as robust SMAD1/5 binding events. Our
523 studies also examined the role of SMAD1/5 in mediating progesterone responses at the genomic and
524 transcription levels. Similarly, our analysis was based on data sets generated from the whole mouse
525 uterus, which contains multiple compartments of the uterine structures, including but not limited to
526 epithelium and stroma. Published studies have shown that nuclear SMAD1/5 localize to the stroma and
527 epithelium during the decidualization process at 4.5 dpc, during the window of implantation[9]. Conditional
528 deletion of SMAD1/5 exclusively in the uterine epithelium using lactoferrin-icre (*Ltf*-icre) results in severe
529 subfertility due to impaired implantation and decidual development[100]. Conditional deletion of SMAD1/5/4
530 exclusively in the cells from mesenchymal lineage (including uterine stroma) using anti-Mullerian
531 hormone type 2 receptor cre (*Amhr2-cre*) results in infertility with defective decidualization[91,92]. Given the
532 essential roles of SMAD1/5 in both stroma and epithelium identified by previous studies, we believe that
533 the transcriptional co-regulatory roles of SMAD1/5 and PR reported here using the whole uterus
534 validates a relationship between SMAD1/5 and PR in both the stromal and epithelial compartments.
535 However, it does not rule out potential co-regulatory roles of SMAD1/5 and PR in the myometrium,
536 immune cells, and/or endothelium, given that whole uterus was used. The specific transcriptional
537 evaluations of SMAD1/5 in the stroma versus the epithelium would require future validations using
538 single-cell sequencing and/or spatial transcriptomic analysis.

539 Although our studies herein confirm that SMAD1 and SMAD5 proteins have distinct transcriptional
540 regulatory activities, our previous studies demonstrated that while SMAD5 can functionally replace
541 SMAD1, SMAD1 cannot replace SMAD5 in the uterus[9]. How this epistatic relationship is established in a

542 tissue-specific manner still needs to be determined by further biochemical investigations. In addition,
543 further studies are needed to uncover whether SMAD1 and SMAD5 response differently upon ligand
544 stimulation in the uterus, and if so, how the preference is achieved. Our study provides versatile *in vivo*
545 genetic tools for these questions and can advance the toolbox for the field studying BMP signaling
546 pathways. Because our mouse models are global knock-in mice, they will not only serve as a powerful
547 tool for studying BMP signaling pathways in the reproductive system but will also promote the study of
548 BMP signaling in other organs and tissues.

549 BMP signaling pathways are involved in a plethora of cellular processes and appropriate functioning of
550 the BMP pathway depends on the precise crosstalk with other signaling pathways. Coordinated
551 communication with other pathways can yield synergistic effects and lead to a complex regulatory
552 network of biological processes. To be specific, SMAD1/5 mediates the crosstalk with the WNT/β-catenin
553 pathway. WNT signaling inhibits glycogen synthase kinase 3β (GSK3β) activity and prevents SMAD1
554 from degradation which governs the embryonic pattern formation[101]. Also, SMAD1/5 can physically
555 interact with T-cell factor (TCF) or lymphoid enhancer factor (LEF) transcription factors to form
556 transcriptional complexes to activate the transcription of many WNT-and BMP-responsive genes[102]. In
557 addition, SMAD1 and SMAD5 can directly associate with Notch intracellular domain and enhance known
558 Notch target gene expression by binding to their regulatory DNA sequences[103]. Intriguingly, in prostate
559 cells, SMAD1 physically interacts with the androgen receptor (AR) and halts the androgen-stimulated
560 prostate cell growth[104]. Moreover, we provide first-hand evidence showing that BMP signaling pathways
561 converge with RA signaling pathways through the regulation of RORB by SMAD1/5. Further studies will
562 grant a more detailed mechanism of the positive feedback loop between BMP and RA signaling.

563 Our previous studies suggest that the mouse endometrium presents decreased P4 responsiveness
564 following the conditional deletion of SMAD1/5 in the uterus[9]. In accordance with the phenotypical
565 observation, we offer compelling support in our current study that SMAD1/5 work collectively with PR to
566 regulate their target genes and that SMAD1/5 mediate the crosstalk between BMP and P4 signaling
567 pathways during decidualization, a key process to ensure a successful pregnancy, and ultimately direct
568 the biological transformations of the uterus during early pregnancy. We provide genomic evidence that
569 SMAD1/5 are co-bound at around 35% of PR target genes in the mouse uterus during decidualization.
570 Correspondingly, in a previously published study where they performed PR ChIP-seq in the mouse
571 uterus after P4 stimulation, the SMAD1 motif was the 5th most significantly enriched sequence motifs
572 identified[35]. In parallel, we also identified nuclear receptor motifs (i.e., PR sequence motifs) enriched in
573 the SMAD1/5 binding sites (Supplement Figure 1D,E). From pathway enrichment analysis, we
574 demonstrate that genes with SMAD1/5 and PR bound at the promoter regions are enriched for key
575 pathways in directing the decidualization process, such as WNT and relaxin signaling pathways. Future

576 studies can benefit from analyzing binding events beyond the promoter regions. Profiling the PR genome
577 occupancy in the SMAD1/5 deficient mice would provide an interesting perspective to reevaluate the
578 major regulatory roles of SMAD1/5 in mediating uterine transcriptomes. In this study, we determined the
579 overlapped transcriptional control between SMAD1/5 and PR at the gene level, and functionally validated
580 the regulatory effect at the transcript level in a human stromal cell decidualization model. While we
581 observe a subset of peak representations that do not overlap at the base pair level in the promoter
582 regions, future functional screenings at the promoter level, such as luciferase reporter assays to assess
583 transcriptional co-activation by SMAD1/5 and PR, will advance this study.

584 SMADs are known to recruit co-repressors (*i.e.*, Ski[105]) or co-activators (*i.e.*, p300[106]) to inhibit or activate
585 target gene transcription, less is known about their cell-specific co-factors that confer the precise spatial-
586 temporal control over binding activities to target genes. Our study highlights the potential co-factors by
587 integrating both genomic and transcriptomic data to delineate signaling crosstalks that are responsible for
588 maintaining tissue homeostasis, especially in the female reproductive tract.

589 Since mice only undergo decidualization upon embryo implantation whilst human stromal cells undergo
590 cyclic decidualization in each menstrual cycle in response to rising levels of progesterone[36],
591 asynchronous gene responses may occur in comparison between mouse models and human cells.
592 However, cellular transformation during decidualization is conserved between mice and humans[32], which
593 makes findings in the mouse models a valuable and transferable resource to be evaluated in human
594 tissues. Accordingly, our functional validation studies were performed using human endometrial stromal
595 cells induced to decidualize *in vitro* for four days, which models the early phases of decidualization.
596 Additional transcriptomic studies of the SMAD1/5 perturbations in human endometrial stromal cells will
597 be of great resource in understanding the entire SMAD1/5 regulomes in humans.

598 In summary, our findings and those of others indicate that SMAD1 and SMAD5 not only are signal
599 transducers for BMP signaling pathways, but also engage extensively in the crosstalk with PR signaling
600 pathways. While P4 responses are critical for early pregnancy establishment, abnormal P4 responses
601 are implicated in diseases such as endometriosis and endometrial cancers[107-110]. Hence, our results
602 which show that BMP and P4 signaling pathways synergize within the endometrium; these key pathways
603 can shed light on the endometrial contribution to conditions that impact reproductive health in women,
604 including early pregnancy loss, endometriosis, and endometrial cancer. Furthermore, we anticipate that
605 the SMAD1/5 knock-in tagged transgenic mouse models developed herein will be useful for studying
606 BMP/SMAD1/5 signaling pathways in other reproductive and non-reproductive tract tissues in the body.

607

DATA AVAILABILITY

Sequencing data and analyses are deposited in the Gene Expression Omnibus under accession number GSE237975. (Reviewer token: gludeooirhczxcj)

SUPPLEMENTARY DATA

Supplementary Table 1: DNA sequences used in the study.
Supplementary Table 2: Direct target genes of SMAD1/5.
Supplementary Table 3: Results of Gene Ontology enrichment analysis of shared direct target genes of SMAD1/5 from the up-targets.
Supplementary Table 4: Results of Gene Ontology enrichment analysis of shared direct target genes of SMAD1/5 from the down-targets.
Supplementary Table 5: Results of KEGG pathway enrichment analysis for shared genes bound by SMAD1, SMAD5, and PR.
Supplementary Table 6: Results of motif analysis results for shared peaks between SMAD1, SMAD5 and PR.
Supplementary Table 7: Gene overlapping results of SMAD1/5 and SOX17.
Supplementary Table 8: Gene overlapping results of SMAD1/5 and NR2F2.
Supplementary File 1: Complete list of motif enrichment analysis from the up-targets and down-targets for SMAD1.
Supplementary File 2: Complete list of motif enrichment analysis from the up-targets and down-targets for SMAD5.
Supplementary Figures: Supplementary Figures 1-3

AUTHOR CONTRIBUTIONS

Zian Liao: Conceptualization, Formal analysis, Methodology, Validation, Writing—original draft. Suni Tang: Data curation, Investigation, Methodology, Visualization, Writing—review & editing. Kaori Nozawa: Data curation, Investigation, Methodology, Writing—review & editing. Keisuke Shimada: Data curation, Methodology, Writing—review & editing. Masahito Ikawa: Project administration, Resources. Diana Monsivais: Conceptualization, Investigation, Supervision, Funding acquisition, Writing – review & editing. Martin M. Matzuk: Conceptualization, Supervision, Funding acquisition, Writing – review & editing.

ACKNOWLEDGEMENTS

FUNDING

This research is supported by Eunice Kennedy Shriver National Institute of Child Health and Human Development grants HD105800 (D.M.), HD096057 (D.M.), HD032067 (M.M.M.), and HD110038 (M.M.M.). DM is supported by a Next Gen Pregnancy Award from the Burroughs Wellcome Fund (NGP10125).

CONFLICT OF INTEREST

No conflict of interest is declared by the authors.

REFERENCE

BIBLIOGRAPHY AND REFERENCES

1 Boivin, J., Bunting, L., Collins, J. A. & Nygren, K. G. International estimates of infertility prevalence and treatment-seeking: potential need and demand for infertility medical care. *Hum Reprod* **22**, 1506-1512, doi:10.1093/humrep/dem046 (2007).

2 Martinez, G. M., Daniels, K. & Febo-Vazquez, I. Fertility of Men and Women Aged 15-44 in the United States: National Survey of Family Growth, 2011-2015. *Natl Health Stat Report*, 1-17 (2018).

3 Wang, X. *et al.* Conception, early pregnancy loss, and time to clinical pregnancy: a population-based prospective study. *Fertil Steril* **79**, 577-584, doi:10.1016/s0015-0282(02)04694-0 (2003).

4 Chang, H., Brown, C. W. & Matzuk, M. M. Genetic analysis of the mammalian transforming growth factor-beta superfamily. *Endocr Rev* **23**, 787-823, doi:10.1210/er.2002-0003 (2002).

5 Monsivais, D., Matzuk, M. M. & Pangas, S. A. The TGF-beta Family in the Reproductive Tract. *Cold Spring Harb Perspect Biol* **9**, doi:10.1101/cshperspect.a022251 (2017).

6 Lee, K. Y. *et al.* Bmp2 is critical for the murine uterine decidual response. *Mol Cell Biol* **27**, 5468-5478, doi:10.1128/MCB.00342-07 (2007).

7 Monsivais, D. *et al.* BMP7 Induces Uterine Receptivity and Blastocyst Attachment. *Endocrinology* **158**, 979-992, doi:10.1210/en.2016-1629 (2017).

8 Nagashima, T. *et al.* BMPR2 is required for postimplantation uterine function and pregnancy maintenance. *J Clin Invest* **123**, 2539-2550, doi:10.1172/JCI65710 (2013).

9 Monsivais, D. *et al.* Endometrial receptivity and implantation require uterine BMP signaling through an ACVR2A-SMAD1/SMAD5 axis. *Nat Commun* **12**, 3386, doi:10.1038/s41467-021-23571-5 (2021).

10 Matzuk, M. M., Kumar, T. R. & Bradley, A. Different phenotypes for mice deficient in either activins or activin receptor type II. *Nature* **374**, 356-360, doi:10.1038/374356a0 (1995).

11 Clementi, C. *et al.* Activin-like kinase 2 functions in peri-implantation uterine signaling in mice and humans. *PLoS Genet* **9**, e1003863, doi:10.1371/journal.pgen.1003863 (2013).

12 Monsivais, D. *et al.* Uterine ALK3 is essential during the window of implantation. *Proc Natl Acad Sci U S A* **113**, E387-395, doi:10.1073/pnas.1523758113 (2016).

13 Teklenburg, G. *et al.* Natural selection of human embryos: decidualizing endometrial stromal cells serve as sensors of embryo quality upon implantation. *PLoS One* **5**, e10258, doi:10.1371/journal.pone.0010258 (2010).

14 Brosens, J. J. *et al.* Uterine selection of human embryos at implantation. *Sci Rep* **4**, 3894, doi:10.1038/srep03894 (2014).
15 Weimar, C. H. *et al.* Endometrial stromal cells of women with recurrent miscarriage fail to discriminate between high- and low-quality human embryos. *PLoS One* **7**, e41424, doi:10.1371/journal.pone.0041424 (2012).
16 Salker, M. S. *et al.* Deregulation of the serum- and glucocorticoid-inducible kinase SGK1 in the endometrium causes reproductive failure. *Nat Med* **17**, 1509-1513, doi:10.1038/nm.2498 (2011).
17 Garrido-Gomez, T. *et al.* Defective decidualization during and after severe preeclampsia reveals a possible maternal contribution to the etiology. *Proc Natl Acad Sci U S A* **114**, E8468-E8477, doi:10.1073/pnas.1706546114 (2017).
18 Garrido-Gomez, T. *et al.* Preeclampsia: a defect in decidualization is associated with deficiency of Annexin A2. *Am J Obstet Gynecol* **222**, 376 e371-376 e317, doi:10.1016/j.ajog.2019.11.1250 (2020).
19 Shimada, K. *et al.* ARMC12 regulates spatiotemporal mitochondrial dynamics during spermiogenesis and is required for male fertility. *Proc Natl Acad Sci U S A* **118**, doi:10.1073/pnas.2018355118 (2021).
20 Fang, B. *et al.* Circadian enhancers coordinate multiple phases of rhythmic gene transcription in vivo. *Cell* **159**, 1140-1152, doi:10.1016/j.cell.2014.10.022 (2014).
21 Skene, P. J. & Henikoff, S. An efficient targeted nuclease strategy for high-resolution mapping of DNA binding sites. *Elife* **6**, doi:10.7554/eLife.21856 (2017).
22 Meers, M. P., Tenenbaum, D. & Henikoff, S. Peak calling by Sparse Enrichment Analysis for CUT&RUN chromatin profiling. *Epigenetics Chromatin* **12**, 42, doi:10.1186/s13072-019-0287-4 (2019).
23 Kent, W. J., Zweig, A. S., Barber, G., Hinrichs, A. S. & Karolchik, D. BigWig and BigBed: enabling browsing of large distributed datasets. *Bioinformatics* **26**, 2204-2207, doi:10.1093/bioinformatics/btq351 (2010).
24 Heinz, S. *et al.* Simple combinations of lineage-determining transcription factors prime cis-regulatory elements required for macrophage and B cell identities. *Mol Cell* **38**, 576-589, doi:10.1016/j.molcel.2010.05.004 (2010).
25 Yu, G., Wang, L. G. & He, Q. Y. ChIPseeker: an R/Bioconductor package for ChIP peak annotation, comparison and visualization. *Bioinformatics* **31**, 2382-2383, doi:10.1093/bioinformatics/btv145 (2015).
26 Ramirez, F. *et al.* deepTools2: a next generation web server for deep-sequencing data analysis. *Nucleic Acids Res* **44**, W160-165, doi:10.1093/nar/gkw257 (2016).
27 Newman, A. M. *et al.* Determining cell type abundance and expression from bulk tissues with digital cytometry. *Nat Biotechnol* **37**, 773-782, doi:10.1038/s41587-019-0114-2 (2019).
28 Initiative, C. Z. (2023).
29 Warren, L. A. *et al.* Analysis of menstrual effluent: diagnostic potential for endometriosis. *Mol Med* **24**, 1, doi:10.1186/s10020-018-0009-6 (2018).
30 Nayyar, A. *et al.* Menstrual Effluent Provides a Novel Diagnostic Window on the Pathogenesis of Endometriosis. *Front Reprod Health* **2**, 3, doi:10.3389/frph.2020.00003 (2020).
31 Martinez-Aguilar, R. *et al.* Menstrual blood-derived stromal cells modulate functional properties of mouse and human macrophages. *Sci Rep* **10**, 21389, doi:10.1038/s41598-020-78423-x (2020).
32 Gellersen, B. & Brosens, J. J. Cyclic decidualization of the human endometrium in reproductive health and failure. *Endocr Rev* **35**, 851-905, doi:10.1210/er.2014-1045 (2014).
33 Magro-Lopez, E. & Munoz-Fernandez, M. A. The Role of BMP Signaling in Female Reproductive System Development and Function. *Int J Mol Sci* **22**, doi:10.3390/ijms222111927 (2021).
34 Li, Q. *et al.* Bone morphogenetic protein 2 functions via a conserved signaling pathway involving Wnt4 to regulate uterine decidualization in the mouse and the human. *J Biol Chem* **282**, 31725-31732, doi:10.1074/jbc.M704723200 (2007).
35 Rubel, C. A. *et al.* Research resource: Genome-wide profiling of progesterone receptor binding in the mouse uterus. *Mol Endocrinol* **26**, 1428-1442, doi:10.1210/me.2011-1355 (2012).

36 Ramathal, C. Y., Bagchi, I. C., Taylor, R. N. & Bagchi, M. K. Endometrial decidualization: of mice and men. *Semin Reprod Med* **28**, 17-26, doi:10.1055/s-0029-1242989 (2010).
37 Wang, S. *et al.* Target analysis by integration of transcriptome and ChIP-seq data with BETA. *Nat Protoc* **8**, 2502-2515, doi:10.1038/nprot.2013.150 (2013).
38 Ciciro, Y. & Sala, A. MYB oncoproteins: emerging players and potential therapeutic targets in human cancer. *Oncogenesis* **10**, 19, doi:10.1038/s41389-021-00309-y (2021).
39 Swartz, C. D., Afshari, C. A., Yu, L., Hall, K. E. & Dixon, D. Estrogen-induced changes in IGF-I, Myb family and MAP kinase pathway genes in human uterine leiomyoma and normal uterine smooth muscle cell lines. *Mol Hum Reprod* **11**, 441-450, doi:10.1093/molehr/gah174 (2005).
40 Akaogi, K. *et al.* KLF4 suppresses estrogen-dependent breast cancer growth by inhibiting the transcriptional activity of ERalpha. *Oncogene* **28**, 2894-2902, doi:10.1038/onc.2009.151 (2009).
41 Timblin, G. A. & Schlissel, M. S. Ebf1 and c-Myb repress rag transcription downstream of Stat5 during early B cell development. *J Immunol* **191**, 4676-4687, doi:10.4049/jimmunol.1301675 (2013).
42 Pan, H., Zhu, L., Deng, Y. & Pollard, J. W. Microarray analysis of uterine epithelial gene expression during the implantation window in the mouse. *Endocrinology* **147**, 4904-4916, doi:10.1210/en.2006-0140 (2006).
43 Fagerberg, L. *et al.* Analysis of the human tissue-specific expression by genome-wide integration of transcriptomics and antibody-based proteomics. *Mol Cell Proteomics* **13**, 397-406, doi:10.1074/mcp.M113.035600 (2014).
44 Ma, W. *et al.* MAX deficiency impairs human endometrial decidualization through down-regulating OSR2 in women with recurrent spontaneous abortion. *Cell Tissue Res* **388**, 453-469, doi:10.1007/s00441-022-03579-z (2022).
45 Rankin, S. A., Gallas, A. L., Neto, A., Gomez-Skarmeta, J. L. & Zorn, A. M. Suppression of Bmp4 signaling by the zinc-finger repressors Osr1 and Osr2 is required for Wnt/beta-catenin-mediated lung specification in Xenopus. *Development* **139**, 3010-3020, doi:10.1242/dev.078220 (2012).
46 Du, H. & Taylor, H. S. The Role of Hox Genes in Female Reproductive Tract Development, Adult Function, and Fertility. *Cold Spring Harb Perspect Med* **6**, a023002, doi:10.1101/cshperspect.a023002 (2015).
47 Cakmak, H. & Taylor, H. S. Molecular mechanisms of treatment resistance in endometriosis: the role of progesterone-hox gene interactions. *Semin Reprod Med* **28**, 69-74, doi:10.1055/s-0029-1242996 (2010).
48 Taylor, H. S., Bagot, C., Kardana, A., Olive, D. & Arici, A. HOX gene expression is altered in the endometrium of women with endometriosis. *Hum Reprod* **14**, 1328-1331, doi:10.1093/humrep/14.5.1328 (1999).
49 He, B., Ni, Z. L., Kong, S. B., Lu, J. H. & Wang, H. B. Homeobox genes for embryo implantation: From mouse to human. *Animal Model Exp Med* **1**, 14-22, doi:10.1002/ame2.12002 (2018).
50 Illingworth, I. M. *et al.* Desmosomes are reduced in the mouse uterine luminal epithelium during the preimplantation period of pregnancy: a mechanism for facilitation of implantation. *Biol Reprod* **63**, 1764-1773, doi:10.1095/biolreprod63.6.1764 (2000).
51 Paria, B. C., Zhao, X., Das, S. K., Dey, S. K. & Yoshinaga, K. Zonula occludens-1 and E-cadherin are coordinately expressed in the mouse uterus with the initiation of implantation and decidualization. *Dev Biol* **208**, 488-501, doi:10.1006/dbio.1999.9206 (1999).
52 Potter, S. W., Gaza, G. & Morris, J. E. Estradiol induces E-cadherin degradation in mouse uterine epithelium during the estrous cycle and early pregnancy. *J Cell Physiol* **169**, 1-14, doi:10.1002/(SICI)1097-4652(199610)169:1<1::AID-JCP1>3.0.CO;2-S (1996).
53 Grund, S. & Grummer, R. Direct Cell(-)Cell Interactions in the Endometrium and in Endometrial Pathophysiology. *Int J Mol Sci* **19**, doi:10.3390/ijms19082227 (2018).
54 Schatz, F., Guzeloglu-Kayisli, O., Arlier, S., Kayisli, U. A. & Lockwood, C. J. The role of decidual cells in uterine hemostasis, menstruation, inflammation, adverse pregnancy outcomes and abnormal uterine bleeding. *Hum Reprod Update* **22**, 497-515, doi:10.1093/humupd/dmw004 (2016).

55 Evans, J. *et al.* Fertile ground: human endometrial programming and lessons in health and disease. *Nat Rev Endocrinol* **12**, 654-667, doi:10.1038/nrendo.2016.116 (2016).
56 Stehlin-Gaon, C. *et al.* All-trans retinoic acid is a ligand for the orphan nuclear receptor ROR beta. *Nat Struct Biol* **10**, 820-825, doi:10.1038/nsb979 (2003).
57 Spitzer, T. L. *et al.* Perivascular human endometrial mesenchymal stem cells express pathways relevant to self-renewal, lineage specification, and functional phenotype. *Biol Reprod* **86**, 58, doi:10.1095/biolreprod.111.095885 (2012).
58 Yin, Y., Haller, M. E., Chadchan, S. B., Kommagani, R. & Ma, L. Signaling through retinoic acid receptors is essential for mammalian uterine receptivity and decidualization. *JCI Insight* **6**, doi:10.1172/jci.insight.150254 (2021).
59 Chang, C. Agonists and Antagonists of TGF-beta Family Ligands. *Cold Spring Harb Perspect Biol* **8**, doi:10.1101/cshperspect.a021923 (2016).
60 Fullerton, P. T., Jr., Monsivais, D., Kommagani, R. & Matzuk, M. M. Follistatin is critical for mouse uterine receptivity and decidualization. *Proc Natl Acad Sci U S A* **114**, E4772-E4781, doi:10.1073/pnas.1620903114 (2017).
61 Li, Q. *et al.* The antiproliferative action of progesterone in uterine epithelium is mediated by Hand2. *Science* **331**, 912-916, doi:10.1126/science.1197454 (2011).
62 Filant, J., DeMayo, F. J., Pru, J. K., Lydon, J. P. & Spencer, T. E. Fibroblast growth factor receptor two (FGFR2) regulates uterine epithelial integrity and fertility in mice. *Biol Reprod* **90**, 7, doi:10.1095/biolreprod.113.114496 (2014).
63 Lim, W., Bae, H., Bazer, F. W. & Song, G. Stimulatory effects of fibroblast growth factor 2 on proliferation and migration of uterine luminal epithelial cells during early pregnancy. *Biol Reprod* **96**, 185-198, doi:10.1095/biolreprod.116.142331 (2017).
64 Russo, L. A. *et al.* Regulated expression of matrix metalloproteinases, inflammatory mediators, and endometrial matrix remodeling by 17beta-estradiol in the immature rat uterus. *Reprod Biol Endocrinol* **7**, 124, doi:10.1186/1477-7827-7-124 (2009).
65 Tenvergert, E., Gillespie, M. W., Kingma, J. & Klasen, H. Abortion attitudes, 1984-1987-1988: effects of item order and dimensionality. *Percept Mot Skills* **74**, 627-642, doi:10.2466/pms.1992.74.2.627 (1992).
66 Hayashi, K. *et al.* Wnt genes in the mouse uterus: potential regulation of implantation. *Biol Reprod* **80**, 989-1000, doi:10.1095/biolreprod.108.075416 (2009).
67 Yang, M. *et al.* Spatiotemporal insight into early pregnancy governed by immune-featured stromal cells. *Cell* **186**, 4271-4288 e4224, doi:10.1016/j.cell.2023.08.020 (2023).
68 Garcia-Alonso, L. *et al.* Mapping the temporal and spatial dynamics of the human endometrium in vivo and in vitro. *Nat Genet* **53**, 1698-1711, doi:10.1038/s41588-021-00972-2 (2021).
69 PrabhuDas, M. *et al.* Immune mechanisms at the maternal-fetal interface: perspectives and challenges. *Nat Immunol* **16**, 328-334, doi:10.1038/ni.3131 (2015).
70 Guimaraes-Young, A., Neff, T., Dupuy, A. J. & Goodheart, M. J. Conditional deletion of Sox17 reveals complex effects on uterine adenogenesis and function. *Dev Biol* **414**, 219-227, doi:10.1016/j.ydbio.2016.04.010 (2016).
71 Hirate, Y. *et al.* Mouse Sox17 haploinsufficiency leads to female subfertility due to impaired implantation. *Sci Rep* **6**, 24171, doi:10.1038/srep24171 (2016).
72 Wang, X. *et al.* SOX17 regulates uterine epithelial-stromal cross-talk acting via a distal enhancer upstream of Ihh. *Nat Commun* **9**, 4421, doi:10.1038/s41467-018-06652-w (2018).
73 Hollnagel, A., Oehlmann, V., Heymer, J., Ruther, U. & Nordheim, A. Id genes are direct targets of bone morphogenetic protein induction in embryonic stem cells. *J Biol Chem* **274**, 19838-19845, doi:10.1074/jbc.274.28.19838 (1999).
74 Miyazono, K. & Miyazawa, K. Id: a target of BMP signaling. *Sci STKE* **2002**, pe40, doi:10.1126/stke.2002.151.pe40 (2002).
75 Holloran, S. M. *et al.* Reciprocal fine-tuning of progesterone and prolactin-regulated gene expression in breast cancer cells. *Mol Cell Endocrinol* **511**, 110859, doi:10.1016/j.mce.2020.110859 (2020).

76 Dinh, D. T. *et al.* Progesterone receptor mediates ovulatory transcription through RUNX transcription factor interactions and chromatin remodelling. *Nucleic Acids Res*, doi:10.1093/nar/gkad271 (2023).
77 Vasquez, Y. M. *et al.* FOXO1 regulates uterine epithelial integrity and progesterone receptor expression critical for embryo implantation. *PLoS Genet* **14**, e1007787, doi:10.1371/journal.pgen.1007787 (2018).
78 Shi, J. W. *et al.* An IGF1-expressing endometrial stromal cell population is associated with human decidualization. *BMC Biol* **20**, 276, doi:10.1186/s12915-022-01483-0 (2022).
79 Suzuki, A. *et al.* Nanog binds to Smad1 and blocks bone morphogenetic protein-induced differentiation of embryonic stem cells. *Proc Natl Acad Sci U S A* **103**, 10294-10299, doi:10.1073/pnas.0506945103 (2006).
80 Shi, X., Bai, S., Li, L. & Cao, X. Hoxa-9 represses transforming growth factor-beta-induced osteopontin gene transcription. *J Biol Chem* **276**, 850-855, doi:10.1074/jbc.M005955200 (2001).
81 Shi, X., Yang, X., Chen, D., Chang, Z. & Cao, X. Smad1 interacts with homeobox DNA-binding proteins in bone morphogenetic protein signaling. *J Biol Chem* **274**, 13711-13717, doi:10.1074/jbc.274.19.13711 (1999).
82 Feng, X. H. & Derynck, R. Specificity and versatility in tgf-beta signaling through Smads. *Annu Rev Cell Dev Biol* **21**, 659-693, doi:10.1146/annurev.cellbio.21.022404.142018 (2005).
83 Massague, J., Seoane, J. & Wotton, D. Smad transcription factors. *Genes Dev* **19**, 2783-2810, doi:10.1101/gad.1350705 (2005).
84 Derynck, R. & Budi, E. H. Specificity, versatility, and control of TGF-beta family signaling. *Sci Signal* **12**, doi:10.1126/scisignal.aav5183 (2019).
85 Lee, D. K. *et al.* Suppression of ERalpha activity by COUP-TFII is essential for successful implantation and decidualization. *Mol Endocrinol* **24**, 930-940, doi:10.1210/me.2009-0531 (2010).
86 Vasquez, Y. M. *et al.* FOXO1 is required for binding of PR on IRF4, novel transcriptional regulator of endometrial stromal decidualization. *Mol Endocrinol* **29**, 421-433, doi:10.1210/me.2014-1292 (2015).
87 Wu, M., Chen, G. & Li, Y. P. TGF-beta and BMP signaling in osteoblast, skeletal development, and bone formation, homeostasis and disease. *Bone Res* **4**, 16009, doi:10.1038/boneres.2016.9 (2016).
88 van Weerd, J. H. & Christoffels, V. M. The formation and function of the cardiac conduction system. *Development* **143**, 197-210, doi:10.1242/dev.124883 (2016).
89 Whitman, M. Smads and early developmental signaling by the TGFbeta superfamily. *Genes Dev* **12**, 2445-2462, doi:10.1101/gad.12.16.2445 (1998).
90 Middlebrook, B. S., Eldin, K., Li, X., Shivasankaran, S. & Pangas, S. A. Smad1-Smad5 ovarian conditional knockout mice develop a disease profile similar to the juvenile form of human granulosa cell tumors. *Endocrinology* **150**, 5208-5217, doi:10.1210/en.2009-0644 (2009).
91 Pangas, S. A. *et al.* Conditional deletion of Smad1 and Smad5 in somatic cells of male and female gonads leads to metastatic tumor development in mice. *Mol Cell Biol* **28**, 248-257, doi:10.1128/MCB.01404-07 (2008).
92 Rodriguez, A. *et al.* SMAD Signaling Is Required for Structural Integrity of the Female Reproductive Tract and Uterine Function During Early Pregnancy in Mice. *Biol Reprod* **95**, 44, doi:10.1095/biolreprod.116.139477 (2016).
93 Retting, K. N., Song, B., Yoon, B. S. & Lyons, K. M. BMP canonical Smad signaling through Smad1 and Smad5 is required for endochondral bone formation. *Development* **136**, 1093-1104, doi:10.1242/dev.029926 (2009).
94 McReynolds, L. J., Gupta, S., Figueroa, M. E., Mullins, M. C. & Evans, T. Smad1 and Smad5 differentially regulate embryonic hematopoiesis. *Blood* **110**, 3881-3890, doi:10.1182/blood-2007-04-085753 (2007).
95 Consortium, E. P. An integrated encyclopedia of DNA elements in the human genome. *Nature* **489**, 57-74, doi:10.1038/nature11247 (2012).
96 Chen, J. *et al.* Single-molecule dynamics of enhanceosome assembly in embryonic stem cells. *Cell* **156**, 1274-1285, doi:10.1016/j.cell.2014.01.062 (2014).

97 Swinstead, E. E. *et al.* Steroid Receptors Reprogram FoxA1 Occupancy through Dynamic Chromatin Transitions. *Cell* **165**, 593-605, doi:10.1016/j.cell.2016.02.067 (2016).
98 Chen, C. H. *et al.* Determinants of transcription factor regulatory range. *Nat Commun* **11**, 2472, doi:10.1038/s41467-020-16106-x (2020).
99 Arvey, A., Agius, P., Noble, W. S. & Leslie, C. Sequence and chromatin determinants of cell-type-specific transcription factor binding. *Genome Res* **22**, 1723-1734, doi:10.1101/gr.127712.111 (2012).
100 Tang, S., Cope, D. I., Vasquez, Y. M. & Monsivais, D. BMP/SMAD1/5 Signaling in the Endometrial Epithelium Is Essential for Receptivity and Early Pregnancy. *Endocrinology* **163**, doi:10.1210/endocr/bqac043 (2022).
101 Fuentealba, L. C. *et al.* Integrating patterning signals: Wnt/GSK3 regulates the duration of the BMP/Smad1 signal. *Cell* **131**, 980-993, doi:10.1016/j.cell.2007.09.027 (2007).
102 Labbe, E., Letamendia, A. & Attisano, L. Association of Smads with lymphoid enhancer binding factor 1/T cell-specific factor mediates cooperative signaling by the transforming growth factor-beta and wnt pathways. *Proc Natl Acad Sci U S A* **97**, 8358-8363, doi:10.1073/pnas.150152697 (2000).
103 Zavadil, J., Cermak, L., Soto-Nieves, N. & Bottinger, E. P. Integration of TGF-beta/Smad and Jagged1/Notch signalling in epithelial-to-mesenchymal transition. *EMBO J* **23**, 1155-1165, doi:10.1038/sj.emboj.7600069 (2004).
104 Qiu, T., Grizzle, W. E., Oelschlager, D. K., Shen, X. & Cao, X. Control of prostate cell growth: BMP antagonizes androgen mitogenic activity with incorporation of MAPK signals in Smad1. *EMBO J* **26**, 346-357, doi:10.1038/sj.emboj.7601499 (2007).
105 Luo, K. *et al.* The Ski oncoprotein interacts with the Smad proteins to repress TGFbeta signaling. *Genes Dev* **13**, 2196-2206, doi:10.1101/gad.13.17.2196 (1999).
106 Pouponnot, C., Jayaraman, L. & Massague, J. Physical and functional interaction of SMADs and p300/CBP. *J Biol Chem* **273**, 22865-22868, doi:10.1074/jbc.273.36.22865 (1998).
107 Brosens, J. J. & Gellersen, B. Death or survival--progesterone-dependent cell fate decisions in the human endometrial stroma. *J Mol Endocrinol* **36**, 389-398, doi:10.1677/jme.1.02060 (2006).
108 Yilmaz, B. D. & Bulun, S. E. Endometriosis and nuclear receptors. *Hum Reprod Update* **25**, 473-485, doi:10.1093/humupd/dmz005 (2019).
109 Janzen, D. M. *et al.* Progesterone receptor signaling in the microenvironment of endometrial cancer influences its response to hormonal therapy. *Cancer Res* **73**, 4697-4710, doi:10.1158/0008-5472.CAN-13-0930 (2013).
110 MacLean, J. A., 2nd & Hayashi, K. Progesterone Actions and Resistance in Gynecological Disorders. *Cells* **11**, doi:10.3390/cells11040647 (2022).

932 **TABLE AND FIGURES LEGENDS**

Figure 1

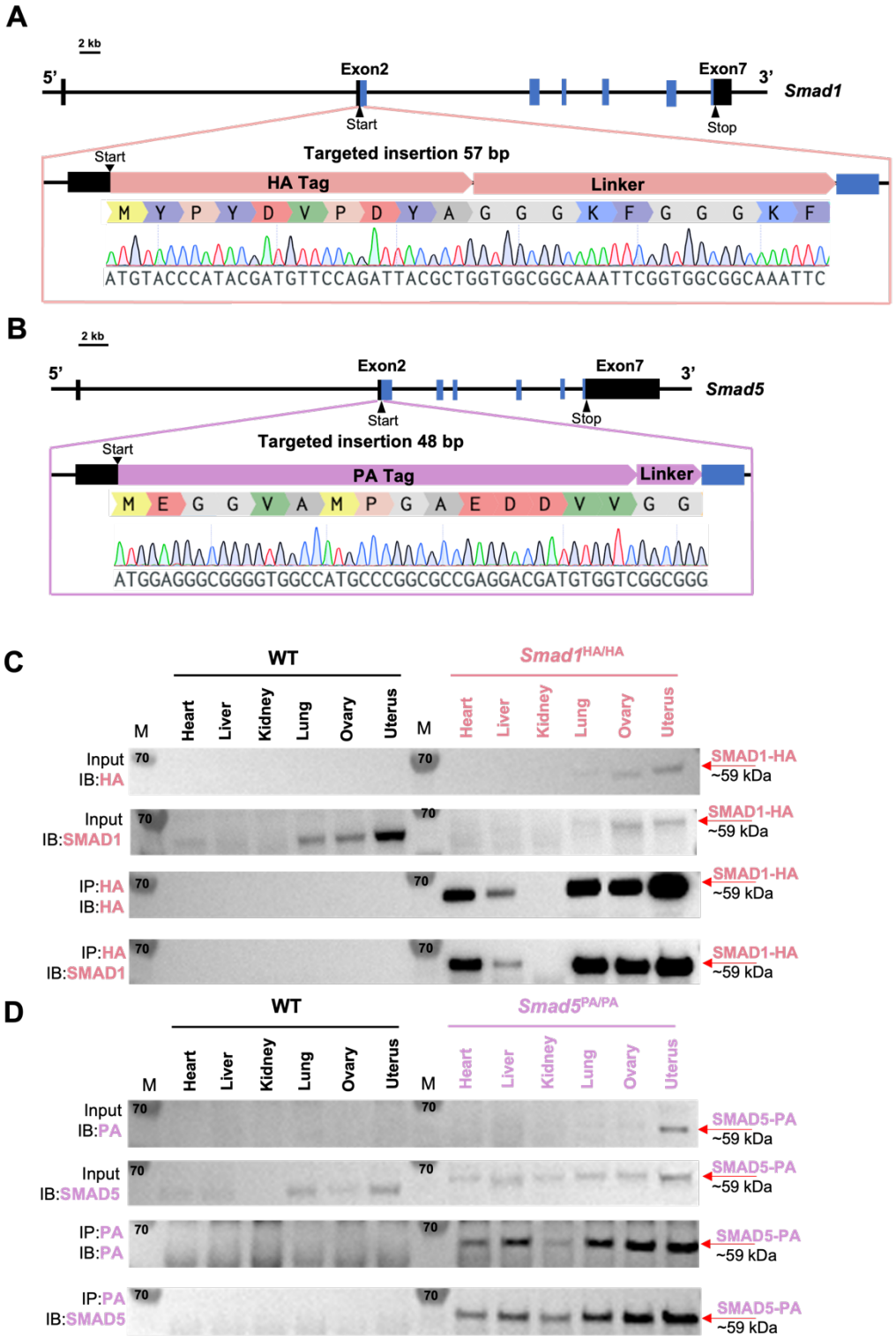

933 **Figure 1: Mouse models with global HA tagged SMAD1 and PA tagged SMAD5 proteins. A-B**)

934 Schematic approaches for generating Smad1HA/HA and Smad5PA/PA knock-in mouse lines. Sanger

935 sequencing of the genotyping results are included as validation of knock-in sequence. Black and blue
936 boxes indicate untranslated and coding regions, respectively. **C-D)** Immunoblot (IB) analysis of the
937 immunoprecipitation (IP) of HA tagged SMAD1 and PA tagged SMAD5 proteins from different tissues of
938 the tagged mouse lines. Wild type (WT) mice were used as negative controls. Antibodies used for IB and
939 IP are as labeled. Targeted bands of SMAD1 and SMAD5 are indicated by red arrows.

Figure 2

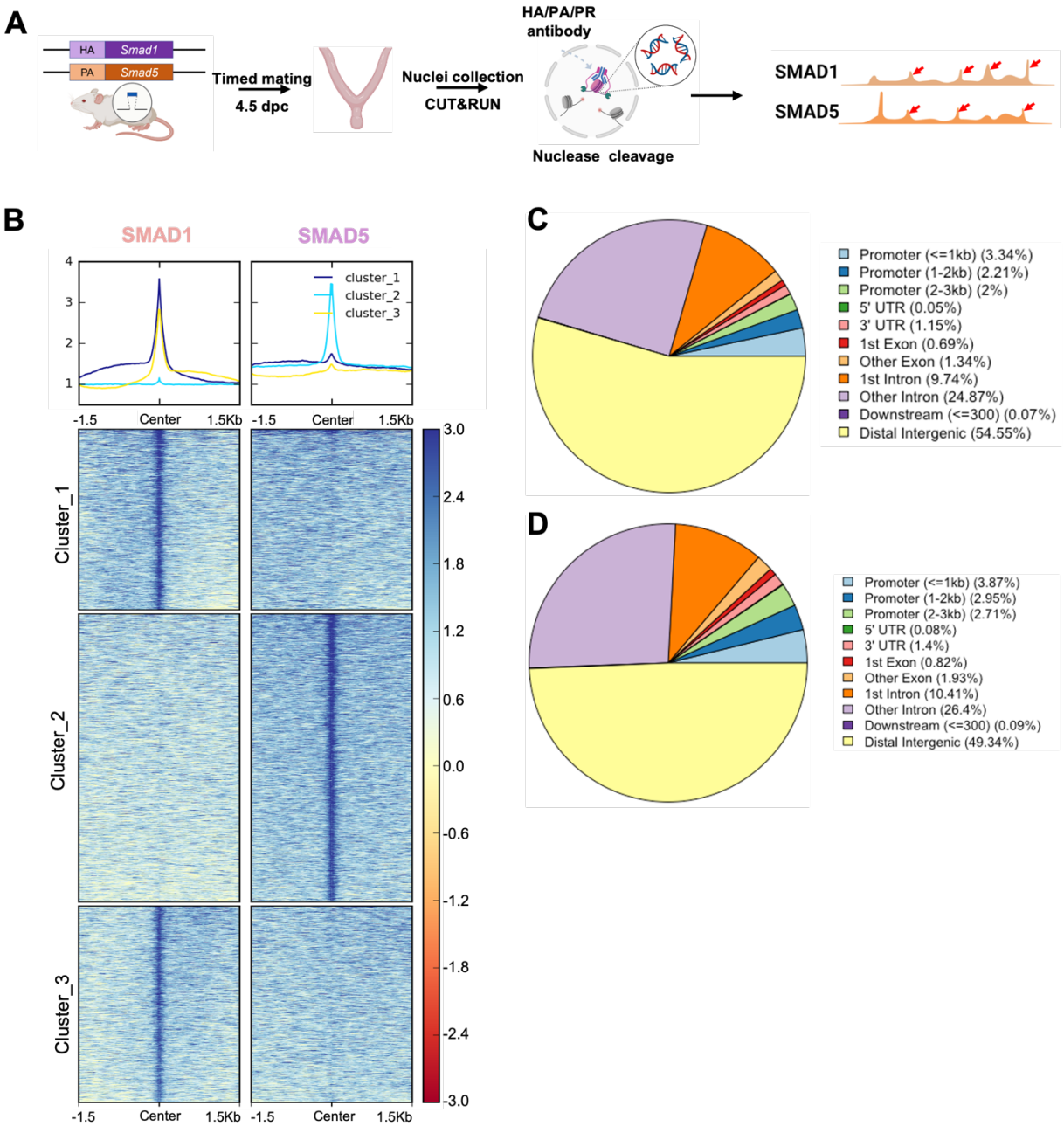

Figure 2: Genomic profiling of SMAD1 and SMAD5 binding sites during decidualization *in vivo*. A) Diagram outlining experimental approaches for tissue collection, processing, and CUT&RUN. **B**) Heatmaps and summary plots showing the enrichment of SMAD1 and SMAD5 binding peaks from one exemplary replicate. Clustering was conducted using k-means algorithm. The colors in the summary plots correspond to clusters labeled in the heatmap below. **C-D**) Feature distribution of the annotated peaks for the SMAD1 (C) binding sites and SMAD5 (D) binding sites.

Figure 3

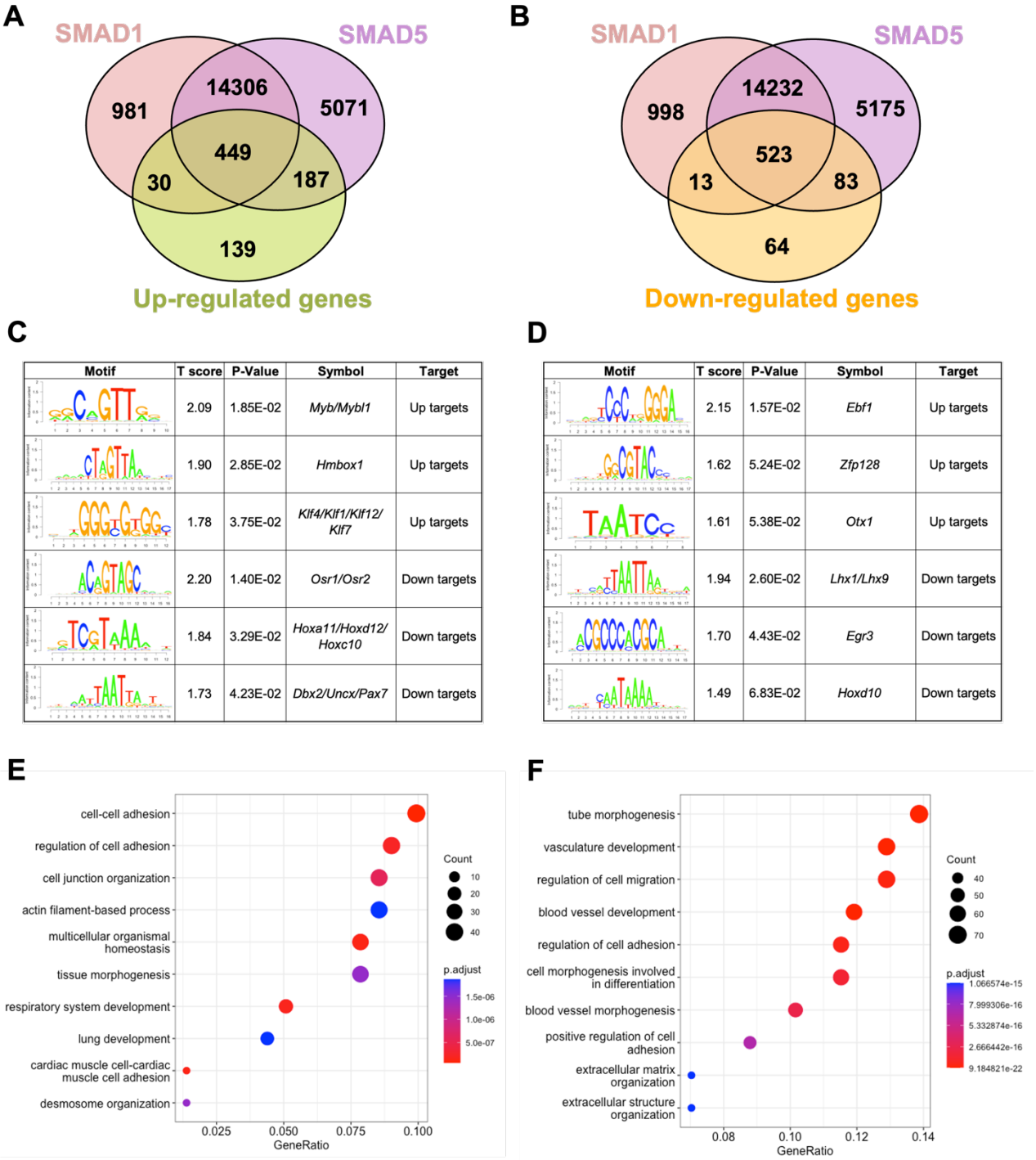

Motif	T score	P-Value	Symbol	Target
	2.09	1.85E-02	*Myb/Mybl1*	Up targets
	1.90	2.85E-02	*Hmbox1*	Up targets
	1.78	3.75E-02	*Klf4/Klf1/Klf12/ Klf7*	Up targets
	2.20	1.40E-02	*Osr1/Osr2*	Down targets
	1.84	3.29E-02	*Hoxa11/Hoxd12/ Hoxc10*	Down targets
	1.73	4.23E-02	*Dbx2/Uncx/Pax7*	Down targets

Motif	T score	P-Value	Symbol	Target
	2.15	1.57E-02	*Ebf1*	Up targets
	1.62	5.24E-02	*Zfp128*	Up targets
	1.61	5.38E-02	*Otx1*	Up targets
	1.94	2.60E-02	*Lhx1/Lhx9*	Down targets
	1.70	4.43E-02	*Egr3*	Down targets
	1.49	6.83E-02	*Hoxd10*	Down targets

Figure 3: SMAD1 and SMAD5 show unique direct target genes during early pregnancy. A-B) Venn diagrams showing the shared and unique direct up-target genes (A) and down-target genes (B) of SMAD1, SMAD5 Numbers indicate genes numbers. **C-D**) Motif enrichment analysis from the up-targets and down-targets for SMAD1 (C) and SMAD5 (D). **E-F**) Dot plot showing Gene Ontology enrichment

950 analysis of shared direct target genes of SMAD1/5 from the up-targets (E) and the down-targets (F),
951 respectively. Dot size represents the gene ratio in the enriched categories compared to background
952 genes, dot colors reflect P-value.

953

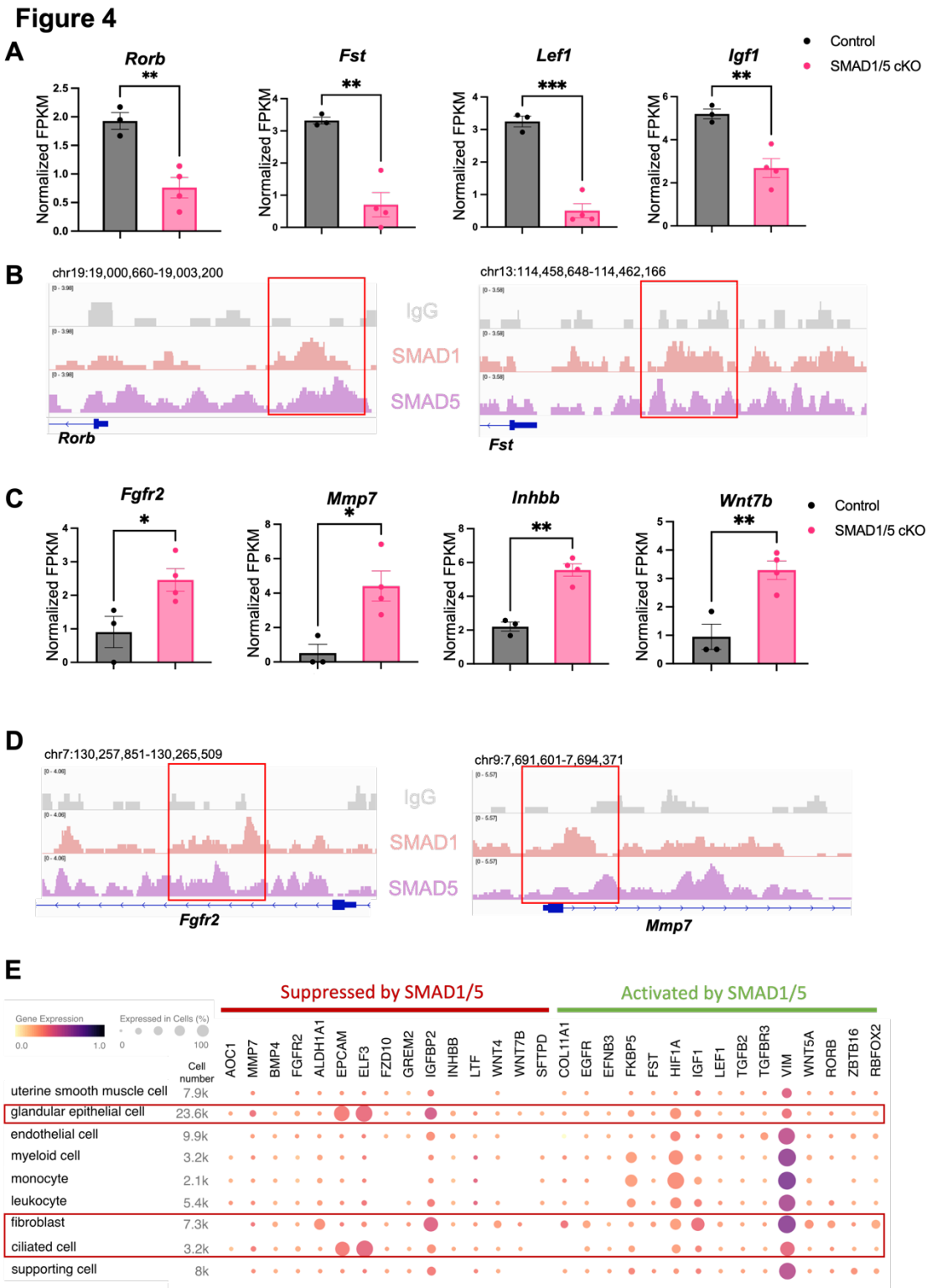

Figure 4: Direct target genes of SMAD1/5 mediate uterine homeostasis. **A**) Bar graph of normalized Fragments Per Kilobase of transcript per Million mapped reads (FPKM) of downregulated transcripts in the Control and SMAD1/5 cKO groups as indicated by the label. Histograms represent average +/- SEM of experiments uteri from Control mice (N=3) and SMAD1/5 cKO mice (N=4). Analyzed by an unpaired t-

958 test. **B**) Integrative Genomics Viewer (IGV) track view of SMAD1, SMAD5 binding activities. Gene loci
959 are as indicated in the figure, genomic coordinates are annotated in mm10. **C**) Bar graph of FPKM of up
960 regulated transcripts in the Control and SMAD1/5 cKO groups as indicated by the label. **D**) IGV track
961 view of SMAD1, SMAD5 binding activities. Gene loci are as indicated in the figure, genomic coordinates
962 are annotated in mm10. **E**) Dot plot showing the gene expression pattern of the key SMAD1/5 direct
963 target genes in different cell types from published human endometrium single-cell RNA-seq dataset.

Figure 5

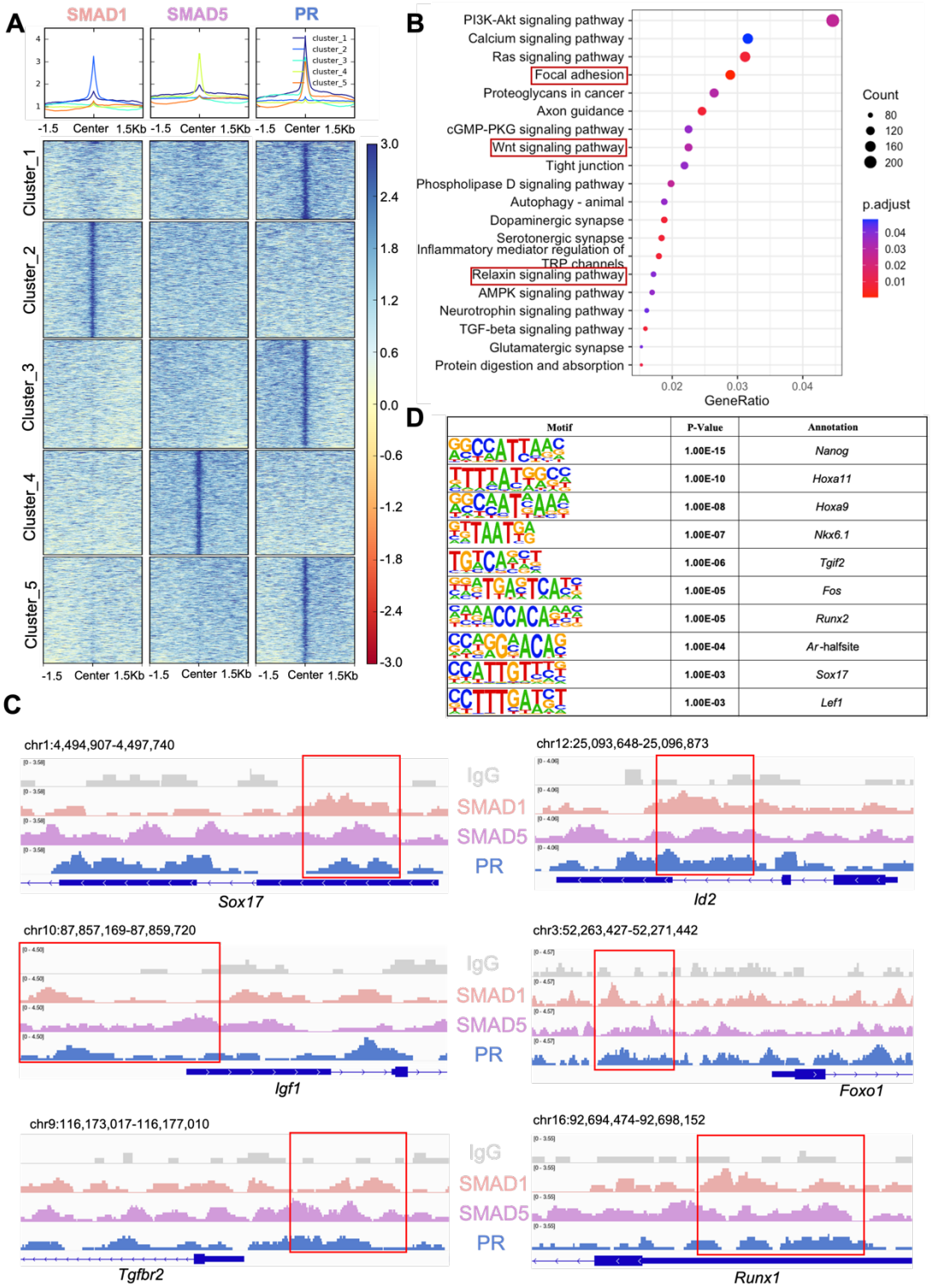

964

965 **Figure 5: SMAD1 and SMAD5 co-regulate PR target genes. A**) Heatmaps and summary plots

966 showing the enrichment comparison between SMAD1, SMAD5 and PR binding peaks from one

967 exemplary replicate. Clustering was conducted using k-means algorithm. The colors in the summary

968 plots correspond to clusters labeled in the heatmap below. **B**) Dot plot showing KEGG pathway
969 enrichment analysis for shared genes bound by SMAD1, SMAD5, and PR. **C**) IGV track view of SMAD1,
970 SMAD5 and PR binding activities. Gene loci are as indicated in the figure, genomic coordinates are
971 annotated in mm10. **D**) Table of motif analysis results for shared peaks between SMAD1, SMAD5 and
972 PR, with P-value and motif annotation specified for each motif.

973

Figure 6

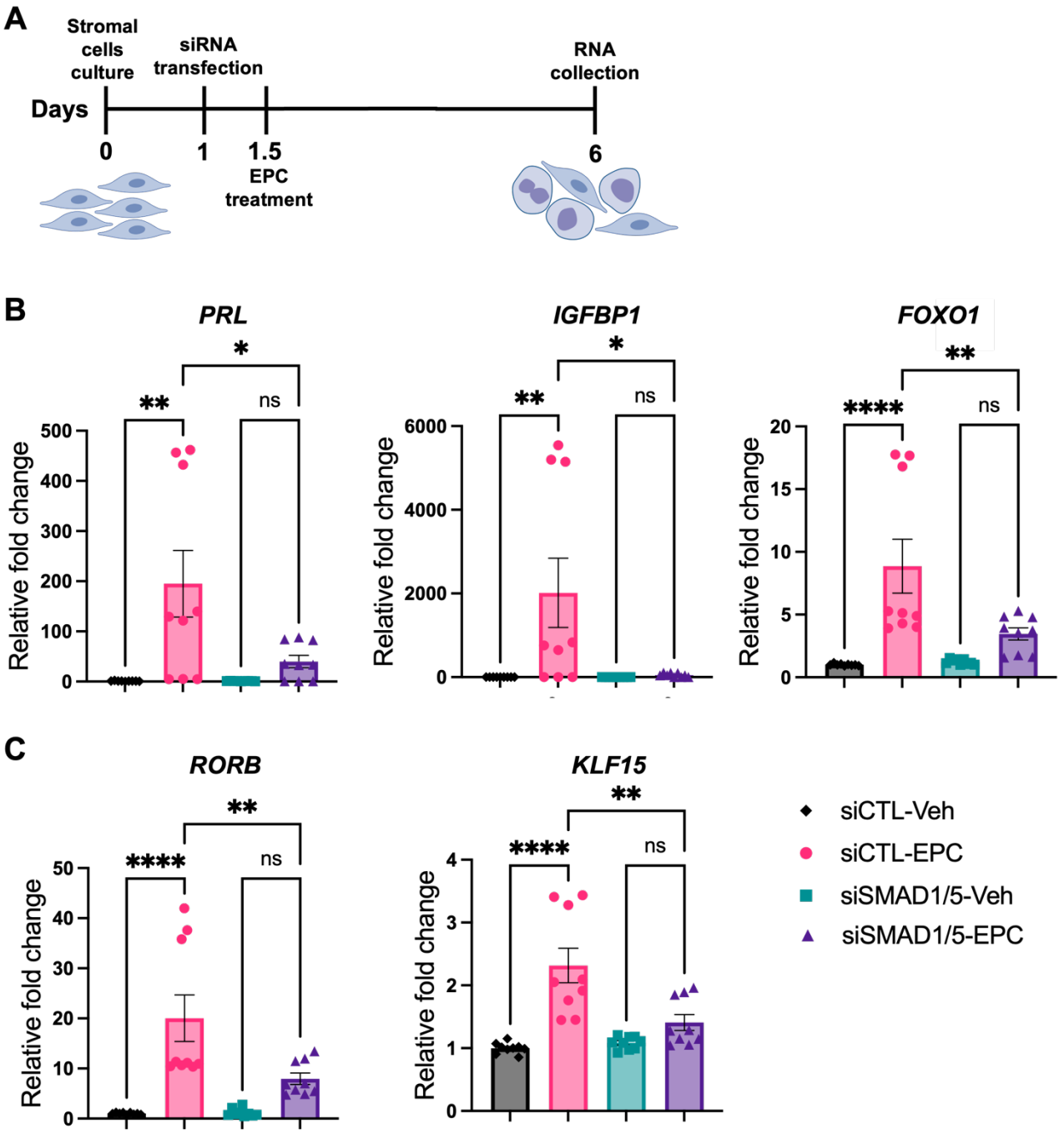

974

975 **Figure 6: SMAD1 and SMAD5 are required for PR responses during decidualization of human**

976 **endometrial stromal cells. A**) Schematic approach and timeline outlining in vitro decidualization for

977 endometrial stromal cells (EnSCs). **B-C**) RT-qPCR results showing mRNA levels of *PRL*, *IGFBP1*,

978 *FOXO1*, *RORB* and *KLF15* after SMAD1/5 perturbation using siRNAs. Data are normalized to siCTL-Veh

979 for visualization. Bar graphs represent average +/- SEM of experiments on cells from three different

980 individuals with technical triplicates. Analyzed by a One-Way ANOVA test with post hoc Tukey test.

Supplement Figure 1:

A

C

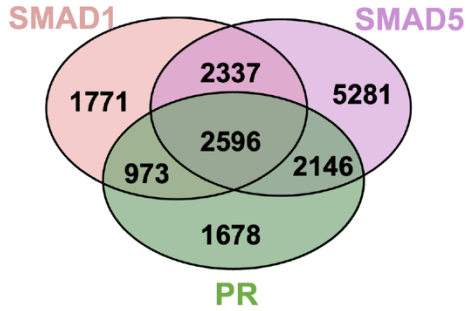

B

	Epithelial cells	Decidual stromal cells	Immune cells	Smooth muscle cells	Placental stromal cells	Endothelial cells	Blood progenitor cells	Mesenchymal stem cell	Trophoblast cells	Allantois	Fetal endothelial cells	Viseral endoderm	Erythroid
Control1	0.0804	0.3112	0.0672	0.0564	0.2196	0.0888	0.1172	0.0039	0.0000	0.0000	0.0000	0.0552	0.0000
Control2	0.0382	0.2632	0.1123	0.0911	0.2202	0.0905	0.0950	0.0543	0.0078	0.0154	0.0020	0.0102	0.0000
Control3	0.0373	0.2688	0.1693	0.0927	0.1959	0.0974	0.0654	0.0479	0.0157	0.0000	0.0000	0.0096	0.0000
KO1	0.2685	0.0299	0.1221	0.0413	0.3804	0.0213	0.0000	0.0439	0.0409	0.0310	0.0031	0.0084	0.0094
KO2	0.1474	0.0878	0.0611	0.0332	0.4830	0.0441	0.0000	0.0197	0.0714	0.0092	0.0000	0.0430	0.0000
KO3	0.1063	0.1406	0.0409	0.0575	0.3290	0.1017	0.1062	0.0369	0.0103	0.0004	0.0000	0.0702	0.0000
KO4	0.1306	0.0705	0.0819	0.0361	0.2114	0.0718	0.1081	0.1435	0.0687	0.0072	0.0010	0.0694	0.0000

Cell fractions: 0.3, 0.2, 0.1, 0

D

Motif	P-Value	Annotation
	1.00E-21	*Mynn*
	1.00E-14	*Trps1*
	1.00E-13	*Hoxa11*
	1.00E-12	*Nanog*
	1.00E-10	*Hoxa9*
	1.00E-09	*Foxa2*
	1.00E-09	*Foxa1*
	1.00E-08	*Isl1*
	1.00E-06	*Pgr*
	1.00E-06	*Ar*-halfsite

E

Motif	P-Value	Annotation
	1E-09	*Cdx2*
	1E-08	*Hoxa9*
	1E-07	*P300*
	0.00001	*Tbet*
	0.00001	*Prop1*
	0.0001	*Scl*
	0.0001	*Ar-halfsite*
	0.001	*Nanog*
	0.001	*Oct4*
	0.01	*Sox6*

F

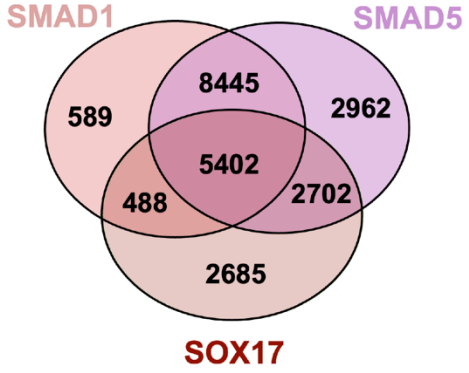

G

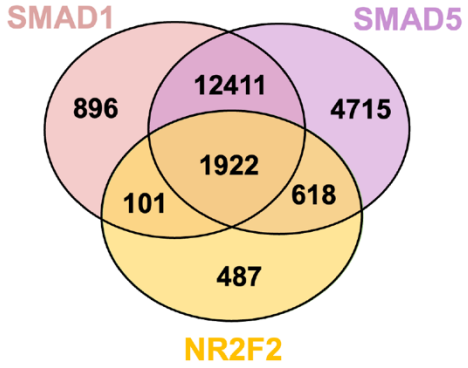

982 **Supplement Figure 1: Gene numbers with SMAD1/5 promoter binding activities and motif**
983 **analysis of SMAD1/5 peaks. A**) Venn diagrams showing the shared and unique genes bound by
984 SMAD1 or SMAD5 in the +/- 3kb region of the promoter regions. **B**) Cell type compositions in the
985 deconvoluted RNA-seq from control mice (Control 1-3) and SMAD1/5 PR-Cre mice (KO1-4). Numbers
986 plotted in the table are absolute values that reflects the absolute proportion of each cell type in the given
987 sample. A larger number indicates a higher proportion of that cell type in the mixture. **C**) Venn diagrams
988 showing the shared and unique genes bound by SMAD1, SMAD5 or PR in the +/- 3kb of the promoter
989 regions. **D-E**) Table of motif analysis results for unique peaks for SMAD1(D) and SMAD5 (E), with P-
990 value and motif annotation specified for each motif. **F)** Venn diagrams showing the shared and unique
991 genes bound by SMAD1, SMAD5 or SOX17 in the +/- 25kb regions near transcription start site. **G)** Venn
992 diagrams showing the shared and unique genes bound by SMAD1, SMAD5 or NR2F2 in the +/- 25kb
993 regions near transcription start site.

Supplement Figure 2:

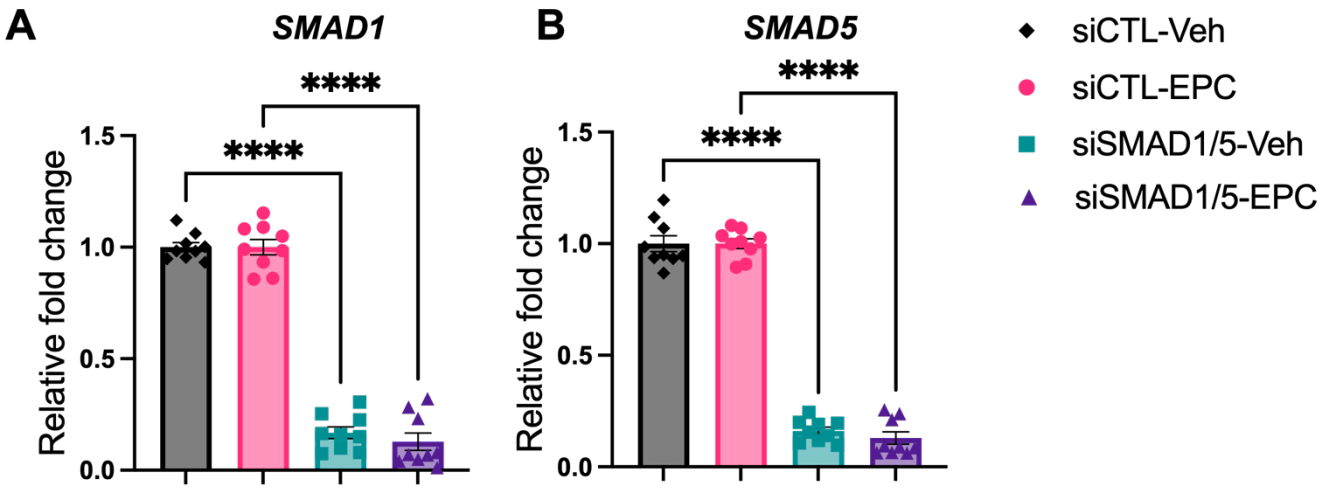

994

995 **Supplement Figure 2: Knockdown effect validation of SMAD1/5 perturbation. A-B**) RT-qPCR
996 results showing mRNA levels of SMAD1(A) and SMAD5 (B) after siRNA treatments in both Veh and EPC
997 conditions. Data are normalized to siCTL for visualization. Bar graphs represent average +/- SEM of
998 experiments on cells from three different individuals with technical triplicates. Analyzed by a One-Way
999 ANOVA test with post hoc Tukey test.

1000

Supplement Figure 3:

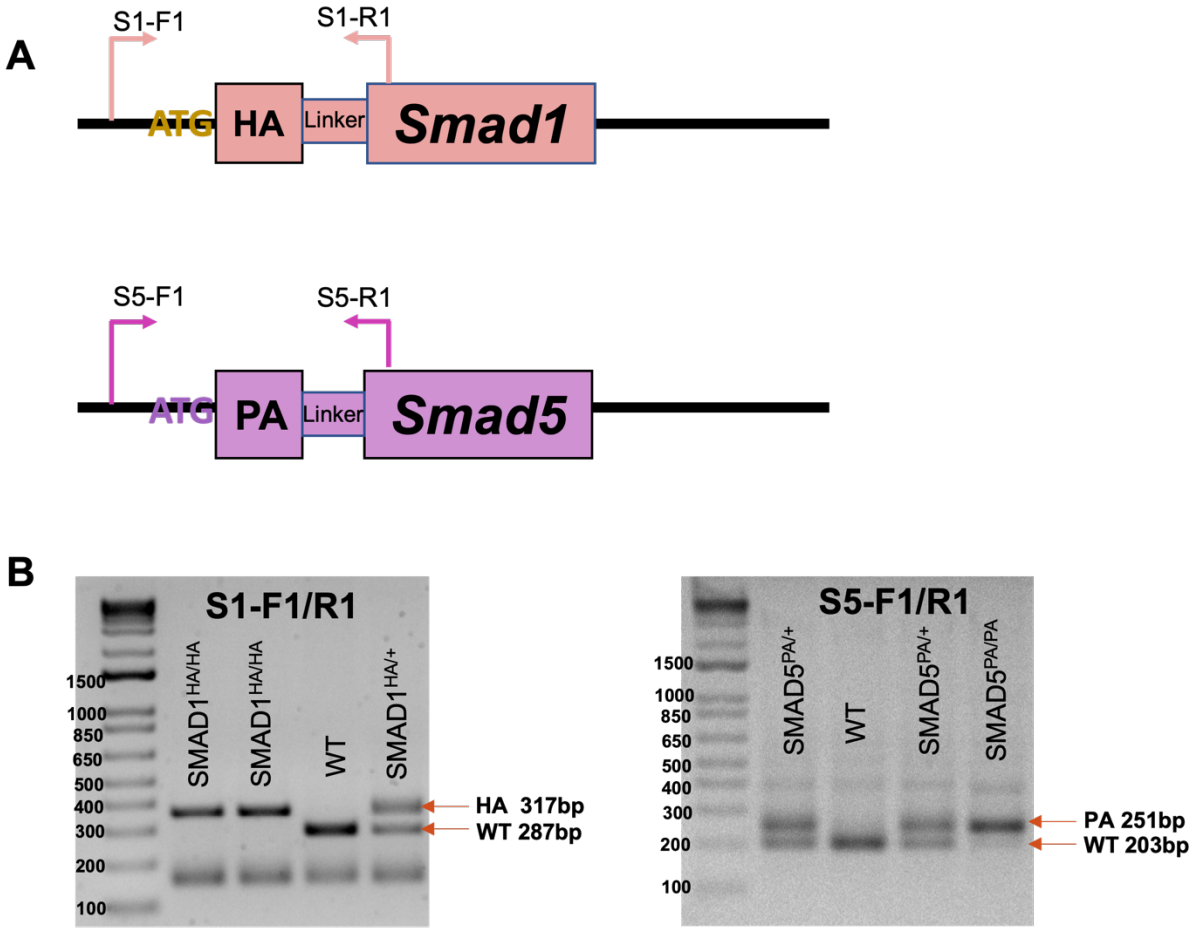

Supplement Figure 3: Genotype of the knock-in mouse lines. **A**) Schematic design of the genotype primers for Smad1HA/HA and Smad5PA/PA mouse lines. **B**) Exemplary gel electrophoresis of PCR products derived from homozygous knock-in mice, heterozygous mice, and WT mice using genotyping primers.

Uncropped Western Blots for Figure 1

A

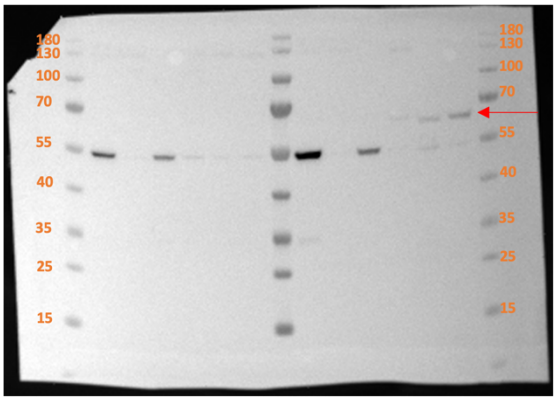

B

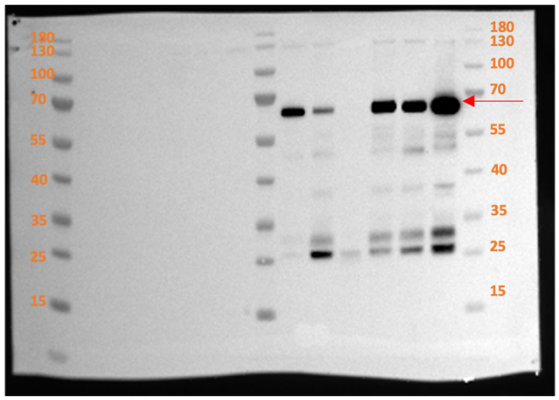

C

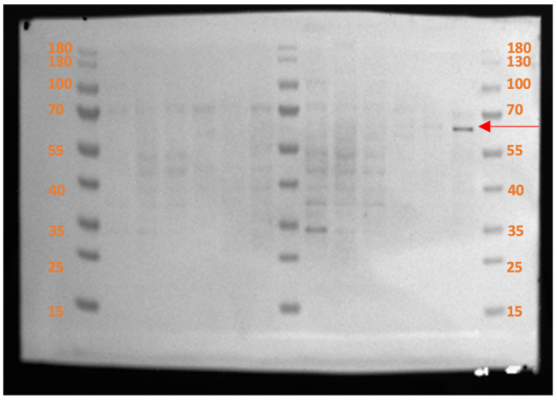

D

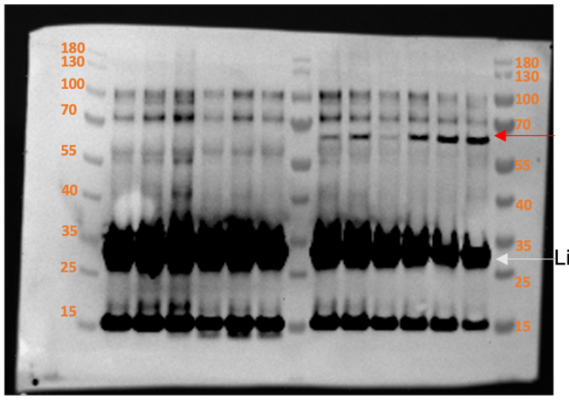

E

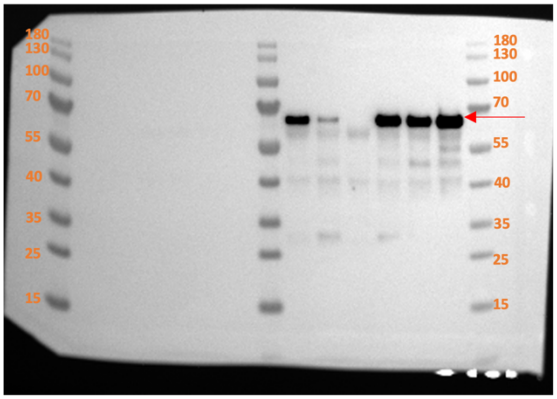
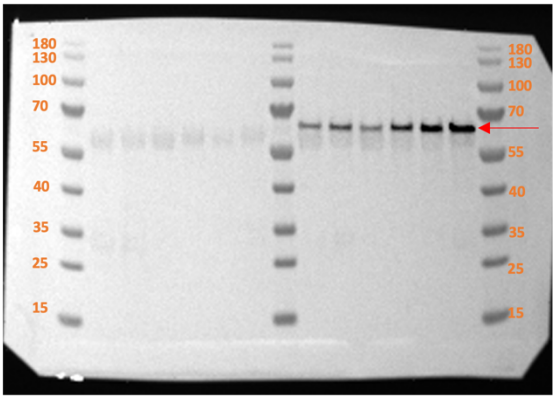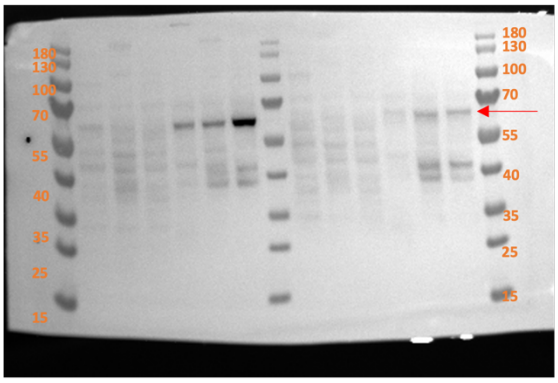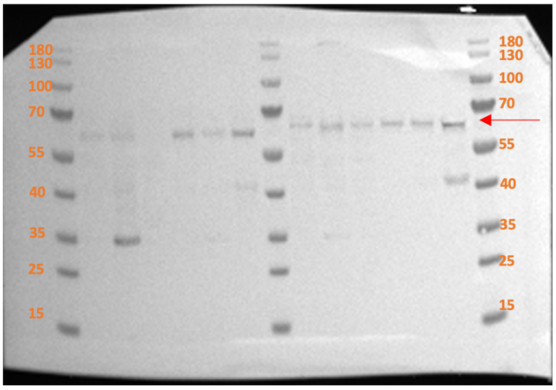
F